Chapter 5
Heptanes-Plus Characterization

5.1 Introduction

Some phase-behavior applications require the use of an equation of state (EOS) to predict properties of petroleum reservoir fluids. The critical properties, acentric factor, molecular weight, and binary-interaction parameters (BIP's) of components in a mixture are required for EOS calculations. With existing chemical-separation techniques, we usually cannot identify the many hundreds and thousands of components found in reservoir fluids. Even if accurate separation were possible, the critical properties and other EOS parameters of compounds heavier than approximately C_{20} would not be known accurately. Practically speaking, we resolve this problem by making an approximate characterization of the heavier compounds with experimental and mathematical methods. The characterization of heptanes-plus (C_{7+}) fractions can be grouped into three main tasks.[1–3]

1. Dividing the C_{7+} fraction into a number of fractions with known molar compositions.
2. Defining the molecular weight, specific gravity, and boiling point of each C_{7+} fraction.
3. Estimating the critical properties and acentric factor of each C_{7+} fraction and the key BIP's for the specific EOS being used.

This chapter presents methods for performing these tasks and gives guidelines on when each method can be used. A unique characterization does not exist for a given reservoir fluid. For example, different component properties are required for different EOS's; therefore, the engineer must determine the quality of a given characterization by testing the predictions of reservoir-fluid behavior against measured pressure/volume/temperature (PVT) data.

The amount of C_{7+} typically found in reservoir fluids varies from >50 mol% for heavy oils to <1 mol% for light reservoir fluids.[4] Average C_{7+} properties also vary widely. For example, C_{7+} molecular weight can vary from 110 to >300 and specific gravity from 0.7 to 1.0. Because the C_{7+} fraction is a mixture of many hundreds of paraffinic, naphthenic, aromatic, and other organic compounds,[5] the C_{7+} fraction cannot be resolved into its individual components with any precision. We must therefore resort to approximate descriptions of the C_{7+} fraction.

Sec. 5.2 discusses experimental methods available for quantifying C_{7+} into discrete fractions. True-boiling-point (TBP) distillation provides the necessary data for complete C_{7+} characterization, including mass and molar quantities, and the key inspection data for each fraction (specific gravity, molecular weight, and boiling point). Gas chromatography (GC) is a less-expensive, time-saving alternative to TBP distillation. However, GC analysis quantifies only the mass of C_{7+} fractions; such properties as specific gravity and boiling point are not provided by GC analysis.

Typically, the practicing engineer is faced with how to characterize a C_{7+} fraction when only $z_{C_{7+}}$ the mole fraction, ; molecular weight, $M_{C_{7+}}$; and specific gravity, $\gamma_{C_{7+}}$, are known. Sec. 5.3 reviews methods for splitting C_{7+} into an arbitrary number of subfractions. Most methods assume that mole fraction decreases exponentially as a function of molecular weight or carbon number. A more general model based on the gamma distribution has been successfully applied to many oil and gas-condensate systems. Other splitting schemes can also be found in the literature; we summarize the available methods.

Sec. 5.4 discusses how to estimate inspection properties γ and T_b for C_{7+} fractions determined by GC analysis or calculated from a mathematical split. Katz and Firoozabadi's[6] generalized single carbon number (SCN) properties are widely used. Other methods for estimating specific gravities of C_{7+} subfractions are based on forcing the calculated $\gamma_{C_{7+}}$ to match the measured value.

Many empirical correlations are available for estimating critical properties of pure compounds and C_{7+} fractions. Critical properties can also be estimated by forcing the EOS to match the boiling point and specific gravity of each C_{7+} fraction separately. In Sec. 5.5, we review the most commonly used methods for estimating critical properties.

Finally, Sec. 5.6 discusses methods for reducing the number of components describing a reservoir mixture and, in particular, the C_{7+} fraction. Splitting the C_{7+} into pseudocomponents is particularly important for EOS-based compositional reservoir simulation. A large part of the computing time during a compositional reservoir simulation is used to solve the flash calculations; accordingly, minimizing the number of components without jeopardizing the quality of the fluid characterization is necessary.

5.2 Experimental Analyses

The most reliable basis for C_{7+} characterization is experimental data obtained from high-temperature distillation or GC. Many experimental procedures are available for performing these analyses; in the following discussion, we review the most commonly used methods. TBP distillation provides the key data for C_{7+} characterization, including mass and molar quantities, specific gravity, molecular weight, and boiling point of each distillation cut. Other such inspection data as kinematic viscosity and refractive index also may be measured on distillation cuts.

Simulated distillation by GC requires smaller samples and less time than TBP distillation.[7-9] However, GC analysis measures only the mass of carbon-number fractions. Simulated distillation results can be calibrated against TBP data, thus providing physical properties for the individual fractions. For many oils, simulated distillation

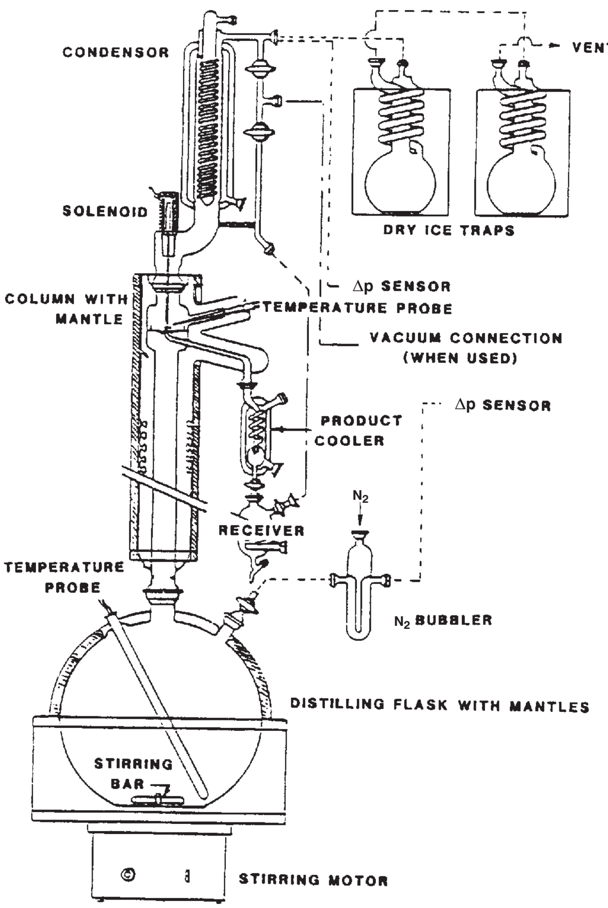

Fig. 5.1—Standard apparatus for conducting TBP analysis of crude-oil and condensate samples at atmospheric and subatmospheric pressures (after Ref. 11).

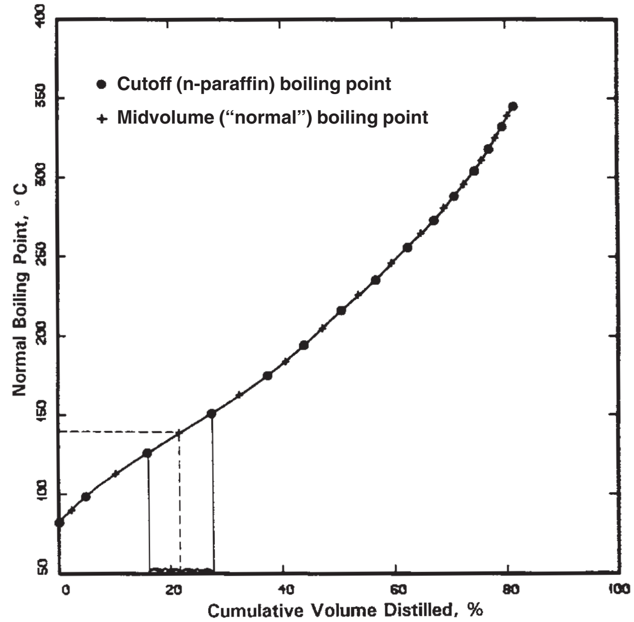

Fig. 5.2—TBP curve for a North Sea gas-condensate sample illustrating the midvolume-point method for calculating average boiling point (after Austad *et al.*[7]).

provides the necessary information for C_{7+} characterization in far less the time and at far less cost than that required for a complete TBP analysis. We recommend, however, that at least one complete TBP analysis be measured for (1) oil reservoirs that may be candidates for gas injection and (2) most gas-condensate reservoirs.

5.2.1 TBP Distillation. In TBP distillation, a stock-tank liquid (oil or condensate) is separated into fractions or "cuts" by boiling-point range. TBP distillation differs from the Hempel and American Soc. for Testing Materials (ASTM) *D-158* distillations[10] because TBP analysis requires a high degree of separation, which is usually controlled by the number of theoretical trays in the apparatus and the reflux ratio. TBP fractions are often treated as components having unique boiling points, critical temperatures, critical pressures, and other properties identified for pure compounds. This treatment is obviously more valid for a cut with a narrow boiling-point range.

The ASTM *D-2892*[11] procedure is a useful standard for TBP analysis of stock-tank liquids. ASTM *D-2892* specifies the general procedure for TBP distillation, including equipment specifications (see **Fig. 5.1**), reflux ratio, sample size, and calculations necessary to arrive at a plot of cumulative volume percent vs. normal boiling point. Normal boiling point implies that boiling point is measured at normal or atmospheric pressure. In practice, to avoid thermal decomposition (cracking), distillation starts at atmospheric pressure and is changed to subatmospheric distillation after reaching a limiting temperature. Subatmospheric boiling-point temperatures are converted to normal boiling-point temperatures by use of a vapor-pressure correlation that corrects for the amount of vacuum and the fraction's chemical composition. The boiling-point range for fractions is not specified in the ASTM standard. Katz and Firoozabadi[6] recommend use of paraffin normal boiling points (plus 0.5°C) as boundaries, a practice that has been widely accepted.

Fig. 5.2[7] shows a plot of typical TBP data for a North Sea sample. Normal boiling point is plotted vs. cumulative volume percent. **Table 5.1** gives the data, including measured specific gravities and molecular weights. Average boiling point is usually taken as the value found at the midvolume percent of a cut. For example, the third cut in Table 5.1 boils from 258.8 to 303.8°F, with an initial 27.49 vol% and a final 37.56 vol%. The midvolume percent is $(27.49+37.56)/2=32.5$ vol%; from Fig. 5.2, the boiling point at this volume is ≈282°F. For normal-paraffin boiling-point intervals, Katz and Firoozabadi's[6] average boiling points of SCN fractions can be used (see **Table 5.2**).

The mass, m_i, of each distillation cut is measured directly during a TBP analysis. The cut is quantified in moles n_i with molecular weight, M_i, and the measured mass m_i, where $n_i = m_i/M_i$. Volume of the fraction is calculated from the mass and the density, ρ_i (or specific gravity, γ_i), where $V_i = m_i/\rho_i$. M_i is measured by a cryoscopic method based on freezing-point depression, and ρ_i is measured by a pycnometer or electronic densitometer. Table 5.1 gives cumulative weight, mole, and volume percents for the North Sea sample. Average C_{7+} properties are given by

$$M_{C_{7+}} = \frac{\sum_{i=1}^{N} m_i}{\sum_{i=1}^{N} n_i}$$

$$\text{and } \rho_{C_{7+}} = \frac{\sum_{i=1}^{N} m_i}{\sum_{i=1}^{N} V_i}, \qquad (5.1)$$

where $\rho_{C_{7+}} = \gamma_{C_{7+}}\rho_w$ with ρ_w = pure water density at standard conditions. These calculated averages are compared with measured values of the C_{7+} sample, and discrepancies are reported as "lost" material.

Refs. 7 and 15 through 20 give procedures for calculating properties from TBP analyses. Also, the ASTM *D-2892*[11] procedure gives details on experimental equipment and the procedure for conducting TBP analysis at atmospheric and subatmospheric conditions. **Table 5.3** gives an example TBP analysis from a commercial laboratory.

TABLE 5.1—EXPERIMENTAL TBP RESULTS FOR A NORTH SEA CONDENSATE

Fraction	Upper T_{bi} (°F)	Average T_{bi}* (°F)	m_i (g)	γ_i**	M_i (g/mol)	V_i (cm^3)	n_i (mol)	w_i (%)	x_{Vi} %	x_i %	Σw_i %	Σx_{Vi} %	K_w
C_7	208.4	194.0	90.2	0.7283	96	123.9	0.940	4.35	4.80	7.80	4.35	4.80	11.92
C_8	258.8	235.4	214.6	0.7459	110	287.7	1.951	10.35	11.15	16.19	14.70	15.95	11.88
C_9	303.8	282.2	225.3	0.7658	122	294.2	1.847	10.87	11.40	15.33	25.57	27.35	11.82
C_{10}	347.0	325.4	199.3	0.7711	137	258.5	1.455	9.61	10.02	12.07	35.18	37.37	11.96
C_{11}	381.2	363.2	128.8	0.7830	151	164.5	0.853	6.21	6.37	7.08	41.40	43.74	11.97
C_{12}	420.8	401.1	136.8	0.7909	161	173.0	0.850	6.60	6.70	7.05	48.00	50.44	12.03
C_{13}	455.0	438.8	123.8	0.8047	181	153.8	0.684	5.97	5.96	5.68	53.97	56.41	11.99
C_{14}	492.8	474.8	120.5	0.8221	193	146.6	0.624	5.81	5.68	5.18	59.78	62.09	11.89
C_{15}	523.4	509.0	101.6	0.8236	212	123.4	0.479	4.90	4.78	3.98	64.68	66.87	12.01
C_{16}	550.4	537.8	74.1	0.8278	230	89.5	0.322	3.57	3.47	2.67	68.26	70.33	12.07
C_{17}	579.2	564.8	76.8	0.8290	245	92.6	0.313	3.70	3.59	2.60	71.96	73.92	12.16
C_{18}	604.4	591.8	58.2	0.8378	259	69.5	0.225	2.81	2.69	1.87	74.77	76.62	12.14
C_{19}	629.6	617.0	50.2	0.8466	266	59.3	0.189	2.42	2.30	1.57	77.19	78.91	12.11
C_{20}	653.0	642.2	45.3	0.8536	280	53.1	0.162	2.19	2.06	1.34	79.37	80.97	12.10
C_{21+}			427.6	0.8708	370	491.1	1.156	20.63	19.03	9.59	100.00	100.00	
Sum			2,073.1			2,580.5	12.049	100.00	100.00	100.00			
Average				0.8034	172								11.98

Reflux ratio = 1 : 5; reflux cycle = 18 seconds; distillation at atmospheric pressure = 201.2 to 347°F; distillation at 100 mm Hg = 347 to 471.2°F; and distillation at 10 mm Hg = 471.2 to 653°F.

$V_i = m_i/\gamma_i/0.9991$; $n_i = m_i/M_i$; $w_i = 100 \times m_i/2073.1$; $x_{Vi} = 100 \times Vi/2580.5$; $x_i = 100 \times n_i/12.049$; $\Sigma w_i = \Sigma w_i$; $\Sigma x_{Vi} = \Sigma x_{Vi}$; and $K_w = (T_{bi}+460)^{1/3}/\gamma_i$.

*Average taken at midvolume point.

**Water = 1.

Boiling points are not reported because normal-paraffin boiling-point intervals are used as a standard; accordingly, the average boiling points suggested by Katz and Firoozabadi[6] (Table 5.2) can be used.

5.2.2 Chromatography. GC and, to a lesser extent, liquid chromatography are used to quantify the relative amount of compounds found in oil and gas systems. The most important application of chromatography to C_{7+} characterization is simulated distillation by GC techniques.

Fig. 5.3 shows an example gas chromatogram for the North Sea sample considered earlier. The dominant peaks are for normal paraffins, which are identified up to n-C_{22}. As a good approximation for a paraffinic sample, the GC response for carbon number C_i starts at the bottom response of n-C_{i-1} and extends to the bottom response of n-C_i. The mass of carbon number C_i is calculated as the area under the curve from the baseline to the GC response in the n-C_{i-1} to n-C_i interval (see the shaded area for fraction C_9 in Fig. 5.3). As **Fig. 5.4**[7] shows schematically, the baseline should be determined before running the actual chromatogram.

Because stock-tank samples cannot be separated completely by standard GC analysis, an internal standard must be used to relate GC area to mass fraction. Normal hexane was used as an internal standard for the sample in Fig. 5.3. The internal standard's response factor may need to be adjusted to achieve consistency between simulated and TBP distillation results. This factor will probably be constant for a given oil, and the factor should be determined on the basis of TBP analysis of at least one sample from a given field. **Fig. 5.5** shows the simulated vs. TBP distillation curves for the Austad *et al.*[7] sample. A 15% correction to the internal-standard response factor was used to match the two distillation curves.

As an alternative to correcting the internal standard, Maddox and Erbar[15] suggest that the reported chromatographic boiling points be adjusted by a correction factor that depends on the reported boiling point and the "paraffinicity" of the composite sample. This correction factor varies from 1 to 1.15 and is slightly larger for aromatic than paraffinic samples.

Several laboratories have calibrated GC analysis to provide simulated-distillation results up to C_{40}. However, checking the accuracy of simulated distillation for SCN fractions greater than approximately C_{25} is difficult because C_{25} is usually the upper limit for reliable TBP distillation. The main disadvantage of simulated distillation is that inspection data are not determined directly for each fraction and must therefore either be correlated from TBP data or estimated from correlations (see Sec. 5.4).

Sophisticated analytical methods, such as mass spectroscopy, may provide detailed information on the compounds separated by GC. For example, mass spectroscopy GC can establish the relative amounts of paraffins, naphthenes, and aromatics (PNA's) for carbon-number fractions distilled by TBP analysis. Detailed PNA information should provide more accurate estimation of the critical properties of petroleum fractions, but the analysis is relatively costly and time-consuming from a practical point of view. Recent work has shown that PNA analysis[3,19-23] may improve C_{7+} characterization for modeling phase behavior with EOS's. Our experience, however, is that PNA data have limited usefulness for improving EOS fluid characterizations.

5.3 Molar Distribution

Molar distribution is usually thought of as the relation between mole fraction and molecular weight. In fact, this concept is misleading because a unique relation does not exist between molecular weight and mole fraction unless the fractions are separated in a consistent manner. Consider for example a C_{7+} sample distilled into 10 cuts separated by normal-paraffin boiling points. If the same C_{7+} sample is distilled with constant 10-vol% cuts, the two sets of data will not

TABLE 5.2—SINGLE CARBON NUMBER PROPERTIES FOR HEPTANES-PLUS (after Katz and Firoozabadi[6])

	Katz-Firoozabadi Generalized Properties							Lee-Kesler[12]/Kesler-Lee[13] Correlations			Riazi[14]	Defined
	T_b Interval*											
Fraction Number	Lower (°F)	Upper (°F)	Average T_b (°F)	Average T_b (°R)	γ*	M	Defined K_w	T_c (°R)	p_c (psia)	ω	V_c (ft³/lbm mol)	Z_c
6	97.7	156.7	147.0	606.7	0.690	84	12.27	914	476	0.271	5.6	0.273
7	156.7	210.0	197.4	657.1	0.727	96	11.96	976	457	0.310	6.2	0.272
8	210.0	259.0	242.1	701.7	0.749	107	11.86	1,027	428	0.349	6.9	0.269
9	259.0	304.3	288.0	747.6	0.768	121	11.82	1,077	397	0.392	7.7	0.266
10	304.3	346.3	330.4	790.1	0.782	134	11.82	1,120	367	0.437	8.6	0.262
11	346.3	385.5	369.0	828.6	0.793	147	11.84	1,158	341	0.479	9.4	0.257
12	385.5	422.2	406.9	866.6	0.804	161	11.86	1,195	318	0.523	10.2	0.253
13	422.2	456.6	441.0	900.6	0.815	175	11.85	1,228	301	0.561	10.9	0.249
14	456.6	489.0	475.5	935.2	0.826	190	11.84	1,261	284	0.601	11.7	0.245
15	489.0	520.0	510.8	970.5	0.836	206	11.84	1,294	268	0.644	12.5	0.241
16	520.0	548.6	541.4	1,001.1	0.843	222	11.87	1,321	253	0.684	13.3	0.236
17	548.6	577.4	572.0	1,031.7	0.851	237	11.87	1,349	240	0.723	14.0	0.232
18	577.4	602.6	595.4	1,055.1	0.856	251	11.89	1,369	230	0.754	14.6	0.229
19	602.6	627.8	617.0	1,076.7	0.861	263	11.90	1,388	221	0.784	15.2	0.226
20	627.8	651.2	640.4	1,100.1	0.866	275	11.92	1,408	212	0.816	15.9	0.222
21	651.2	674.6	663.8	1,123.5	0.871	291	11.94	1,428	203	0.849	16.5	0.219
22	674.6	692.6	685.4	1,145.1	0.876	305	11.94	1,447	195	0.879	17.1	0.215
23	692.6	717.8	707.0	1,166.7	0.881	318	11.95	1,466	188	0.909	17.7	0.212
24	717.8	737.6	726.8	1,186.5	0.885	331	11.96	1,482	182	0.936	18.3	0.209
25	737.6	755.6	746.6	1,206.3	0.888	345	11.99	1,498	175	0.965	18.9	0.206
26	755.6	775.4	766.4	1,226.1	0.892	359	12.00	1,515	168	0.992	19.5	0.203
27	775.4	793.4	786.2	1,245.9	0.896	374	12.01	1,531	163	1.019	20.1	0.199
28	793.4	809.6	804.2	1,263.9	0.899	388	12.03	1,545	157	1.044	20.7	0.196
29	809.6	825.8	820.4	1,280.1	0.902	402	12.04	1,559	152	1.065	21.3	0.194
30	825.8	842.0	834.8	1,294.5	0.905	416	12.04	1,571	149	1.084	21.7	0.191
31	842.0	858.2	851.0	1,310.7	0.909	430	12.04	1,584	145	1.104	22.2	0.189
32	858.2	874.4	865.4	1,325.1	0.912	444	12.04	1,596	141	1.122	22.7	0.187
33	874.4	888.8	879.8	1,339.5	0.915	458	12.05	1,608	138	1.141	23.1	0.185
34	888.8	901.4	892.4	1,352.1	0.917	472	12.06	1,618	135	1.157	23.5	0.183
35	901.4	915.8	906.8	1,366.5	0.920	486	12.06	1,630	131	1.175	24.0	0.180
36			919.4	1,379.1	0.922	500	12.07	1,640	128	1.192	24.5	0.178
37			932.0	1,391.7	0.925	514	12.07	1,650	126	1.207	24.9	0.176
38			946.4	1,406.1	0.927	528	12.09	1,661	122	1.226	25.4	0.174
39			959.0	1,418.7	0.929	542	12.10	1,671	119	1.242	25.8	0.172
40			971.6	1,431.3	0.931	556	12.10	1,681	116	1.258	26.3	0.170
41			982.4	1,442.1	0.933	570	12.11	1,690	114	1.272	26.7	0.168
42			993.2	1,452.9	0.934	584	12.13	1,697	112	1.287	27.1	0.166
43			1,004.0	1,463.7	0.936	598	12.13	1,706	109	1.300	27.5	0.164
44			1,016.6	1,476.3	0.938	612	12.14	1,716	107	1.316	27.9	0.162
45			1,027.4	1,487.1	0.940	626	12.14	1,724	105	1.328	28.3	0.160

*At 1 atmosphere.
**Water = 1.

produce the same plot of mole fraction vs. molecular weight. However, a plot of cumulative mole fraction,

$$Q_{zi} = \frac{\sum_{j=1}^{i} z_j}{\sum_{j=1}^{N} z_j}, \quad \ldots\ldots\ldots\ldots\ldots\ldots\ldots\ldots\ldots\ldots \quad (5.2)$$

vs. cumulative average molecular weight,

$$Q_{Mi} = \frac{\sum_{j=1}^{i} z_j M_j}{\sum_{j=1}^{i} z_j}, \quad \ldots\ldots\ldots\ldots\ldots\ldots\ldots\ldots\ldots\ldots \quad (5.3)$$

TABLE 5.3—STANDARD TBP RESULTS FROM COMMERCIAL PVT LABORATORY

Component	mol%	wt%	Density (g/cm³)	Gravity γ_{API}	Molecular Weight
Heptanes	1.12	2.52	0.7258	63.2	96
Octanes	1.30	3.08	0.7470	57.7	101
Nonanes	1.18	3.15	0.7654	53.1	114
Decanes	0.98	2.96	0.7751	50.9	129
Undecanes	0.62	2.10	0.7808	49.5	144
Dodecanes	0.57	2.18	0.7971	45.8	163
Tridecanes	0.74	3.05	0.8105	42.9	177
Tetradecanes	0.53	2.39	0.8235	40.1	192
Pentadecanes plus	4.10	31.61	0.8736	30.3	330

*At 60°F.
Note: Katz and Firoozabadi[6] average boiling points (Table 5.2) can be used when normal paraffin boiling-point intervals are used.

should produce a single curve. Strictly speaking, therefore, molar distribution is the relation between cumulative molar quantity and some expression for cumulative molecular weight.

In this section, we review methods commonly used to describe molar distribution. Some methods use a consistent separation of fractions (e.g., by SCN) so the molar distribution can be expressed directly as a relationship between mole fraction and molecular weight of individual cuts. Most methods in this category assume that C_{7+} mole fractions decrease exponentially. A more general approach uses the continuous three-parameter gamma probability function to describe molar distribution.

5.3.1 Exponential Distributions. The Lohrenz-Bray-Clark[24] (LBC) viscosity correlation is one of the earliest attempts to use an exponential-type distribution for splitting C_{7+}. The LBC method splits C_{7+} into normal paraffins C_7 though C_{40} with the relation

$$z_i = z_{C_6} \exp[A_1(i-6) + A_2(i-6)^2], \quad \ldots\ldots\ldots\ldots (5.4)$$

where i = carbon number and z_{C_6} = measured C_6 mole fraction. Constants A_1 and A_2 are determined by trial and error so that

$$z_{C_{7+}} = \sum_{i=7}^{40} z_i \quad \ldots\ldots\ldots\ldots\ldots\ldots\ldots\ldots (5.5)$$

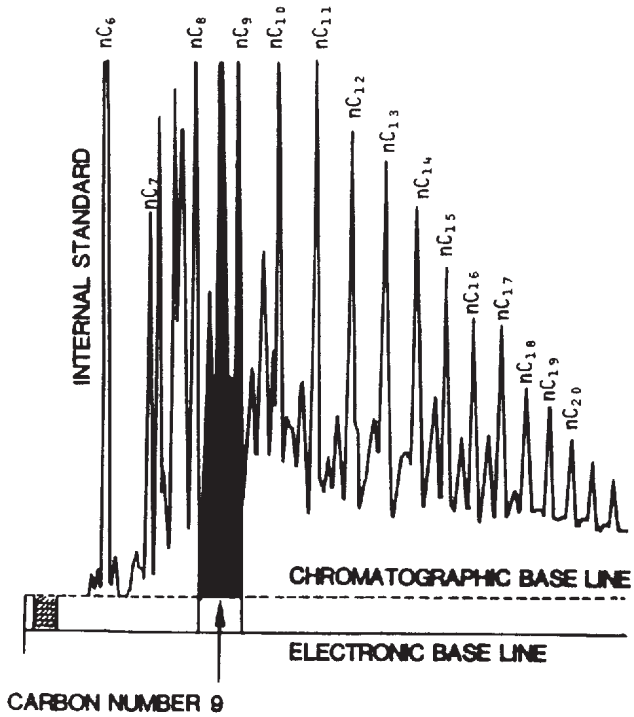

Fig. 5.3—Simulated distillation by GC of the North Sea gas-condensate sample in Fig. 5.2 (after Austad *et al.*[7]).

and $z_{C_{7+}} M_{C_{7+}} = \sum_{i=7}^{40} z_i M_i \quad \ldots\ldots\ldots\ldots\ldots\ldots\ldots\ldots (5.6)$

are satisfied. Paraffin molecular weights ($M_i = 14i + 2$) are used in Eq. 5.6. A Newton-Raphson algorithm can be used to solve Eqs. 5.5 and 5.6. Note that the LBC model cannot be used when $z_{C_{7+}} < z_{C_6}$ and $M_{C_{7+}} > M_{C_{40}}$. The LBC form of the exponential distribution has not found widespread application.

More commonly, a linear form of the exponential distribution is used to split the C_{7+} fraction. Writing the exponential distribution in a general form for any C_{n+} fraction ($n = 7$ being a special case),

$$z_i = z_{C_n} \exp A[(i-n)], \quad \ldots\ldots\ldots\ldots\ldots\ldots\ldots\ldots (5.7)$$

where i = carbon number, z_{C_n} = mole fraction of C_n, and A = constant indicating the slope on a plot of $\ln z_i$ vs. i. The constants z_{C_n} and A can be determined explicitly. With the general expression

$$M_i = 14i + h \quad \ldots\ldots\ldots\ldots\ldots\ldots\ldots\ldots\ldots\ldots (5.8)$$

for molecular weight of C_i and the assumption that the distribution is infinite, constants z_{C_n} and A are given by

$$z_{C_n} = \frac{14}{M_{C_{n+}} - 14(n-1) - h} \quad \ldots\ldots\ldots\ldots\ldots\ldots\ldots\ldots (5.9)$$

and $A = \ln\left(1 - z_{C_n}\right) \quad \ldots\ldots\ldots\ldots\ldots\ldots\ldots\ldots\ldots\ldots (5.10)$

so that $\sum_{i=n}^{\infty} z_i = 1 \quad \ldots\ldots\ldots\ldots\ldots\ldots\ldots\ldots\ldots\ldots (5.11)$

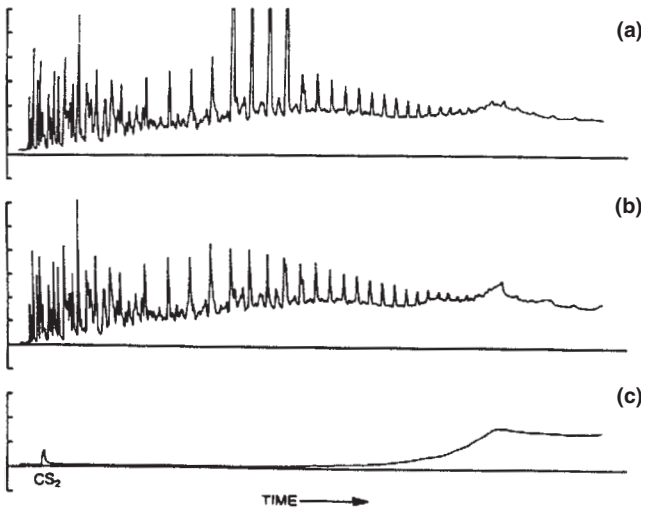

Fig. 5.4—GC simulated distillation chromatograms (a) without any sample (used to determine the baseline), (b) for a crude oil, and (c) for a crude oil with internal standard (after MacAllister and DeRuiter[9]).

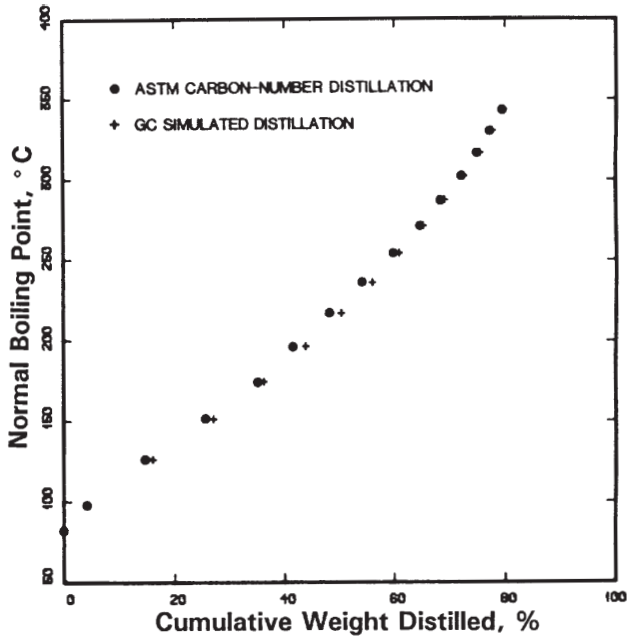

Fig. 5.5—Comparison of TBP and GC-simulated distillation for a North Sea gas-condensate sample (after Austad *et al.*[7]).

$$\text{and} \sum_{i=n}^{\infty} z_i M_i = M_{C_{n+}} \quad \ldots\ldots\ldots\ldots\ldots\ldots\ldots\ldots \quad (5.12)$$

are satisfied.

Eqs. 5.9 and 5.10 imply that once a molecular weight relation is chosen (i.e., h is fixed), the distribution is uniquely defined by C_{7+} molecular weight. Realistically, all reservoir fluids having a given C_{7+} molecular weight will not have the same molar distribution, which is one reason why more complicated models have been proposed.

5.3.2 Gamma-Distribution Model. The three-parameter gamma distribution is a more general model for describing molar distribution. Whitson[2,25,26] and Whitson *et al.*[27] discuss the gamma distribution and its application to molar distribution. They give results for 44 oil and condensate C_{7+} samples that were fit by the gamma distribution with data from complete TBP analyses. The absolute average deviation in estimated cut molecular weight was 2.5 amu (molecular weight units) for the 44 samples.

The gamma probability density function is

$$\mathrm{p}(M) = \frac{(M-\eta)^{\alpha-1}\exp\left\{-\left[(M-\eta)/\beta\right]\right\}}{\beta^{\alpha}\Gamma(\alpha)}, \quad \ldots\ldots\ldots \quad (5.13)$$

where Γ = gamma function and β is given by

$$\beta = \frac{M_{C_{7+}} - \eta}{\alpha}. \quad \ldots\ldots\ldots\ldots\ldots\ldots\ldots\ldots \quad (5.14)$$

The three parameters in the gamma distribution are α, η, and $M_{C_{7+}}$ The key parameter α defines the form of the distribution, and its value usually ranges from 0.5 to 2.5 for reservoir fluids; $\alpha = 1$ gives an exponential distribution. Application of the gamma distribution to heavy oils, bitumen, and petroleum residues indicates that the upper limit for α is 25 to 30, which statistically is approaching a log-normal distribution (see **Fig. 5.6**[28]).

The parameter η can be physically interpreted as the minimum molecular weight found in the C_{7+} fraction. An approximate relation between α and η is

$$\eta \approx \frac{110}{1-(1+4/\alpha^{0.7})} \quad \ldots\ldots\ldots\ldots\ldots\ldots\ldots\ldots \quad (5.15)$$

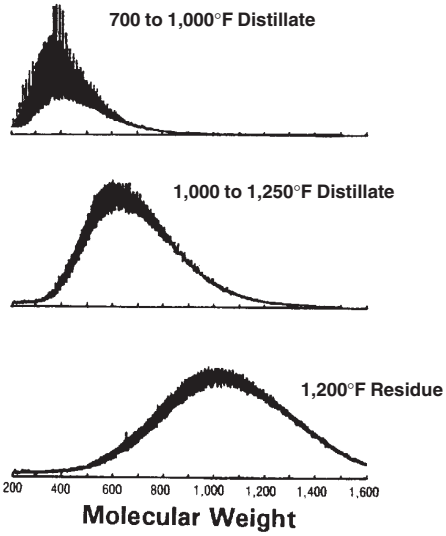

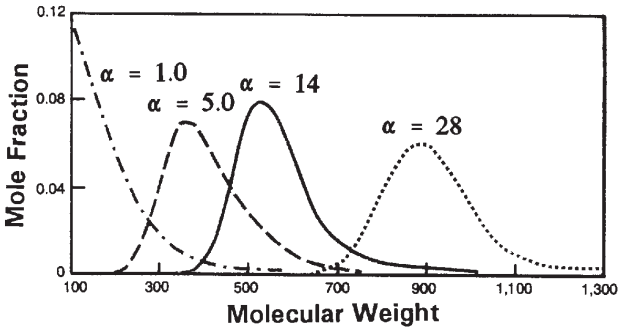

Fig. 5.6—Gamma distributions for petroleum residue (after Brulé *et al.*[28]).

for reservoir-fluid C_{7+} fractions. Practically, η should be considered as a mathematical constant more than as a physical property, either calculated from Eq. 5.15 or determined by fitting measured TBP data.

Fig. 5.7 shows the function p(M) for the Hoffman *et al.*[29] oil and a North Sea oil. Parameters for these two oils were determined by fitting experimental TBP data. The Hoffman *et al.* oil has a relatively large α of 2.27, a relatively small η of 75.7, with $M_{C_{7+}} = 198$; the North Sea oil is described by $\alpha = 0.82$, $\eta = 93.2$, and $M_{C_{7+}} = 227$.

The continuous distribution p(M) is applied to petroleum fractions by dividing the area under the p(M) curve into sections (shown schematically in **Fig. 5.8**). By definition, total area under the p(M) curve from η to ∞ is unity. The area of a section is defined as normalized mole fraction $z_i/z_{C_{7+}}$ for the range of molecular weights M_{bi-1} to M_{bi}. If the area from η to molecular-weight boundary M_b is defined as $P_0(M_b)$, then the area of Section i is $P_0(M_{bi}) - P_0(M_{bi-1})$, also shown schematically in Fig. 5.8. Mole fraction z_i can be written

$$z_i = z_{C_{7+}}\left[P_0\left(M_{bi}\right) - P_0\left(M_{bi-1}\right)\right]. \quad \ldots\ldots\ldots\ldots\ldots \quad (5.16)$$

Average molecular weight in the same interval is given by

$$M_i = \eta + \alpha\beta\frac{P_1\left(M_{bi}\right) - P_1\left(M_{bi-1}\right)}{P_0\left(M_{bi}\right) - P_0\left(M_{bi-1}\right)}, \quad \ldots\ldots\ldots\ldots \quad (5.17)$$

$$\text{where } P_0 = QS, \quad \ldots\ldots\ldots\ldots\ldots\ldots\ldots\ldots \quad (5.18)$$

$$\text{and } P_1 = Q\left(S - \frac{1}{\alpha}\right), \quad \ldots\ldots\ldots\ldots\ldots\ldots\ldots \quad (5.19)$$

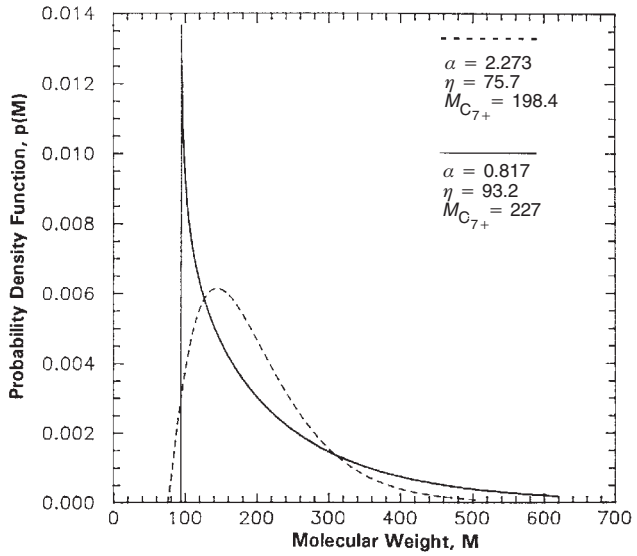

Fig. 5.7—Gamma density function for the Hoffman *et al.*[29] oil (dashed line) and a North Sea volatile oil (solid line). After Whitson *et al.*[27]

$$\text{where } Q = e^{-y} y^{\alpha} \Gamma(\alpha), \quad \ldots\ldots\ldots\ldots\ldots\ldots\ldots\ldots \quad (5.20)$$

$$S = \sum_{j=0}^{\infty} y^{j} \left[\prod_{k=0}^{j} (\alpha + k) \right]^{-1}, \quad \ldots\ldots\ldots\ldots\ldots\ldots \quad (5.21)$$

$$\text{and } y = \frac{M_b - \eta}{\beta}. \quad \ldots\ldots\ldots\ldots\ldots\ldots\ldots\ldots \quad (5.22)$$

Note that $P_0(M_{b0}=\eta) = P_1(M_{b0}=\eta) = 0$.

The summation in Eq. 5.21 should be performed until the last term is $< 1 \times 10^{-8}$. The gamma function can be estimated by[30]

$$\Gamma(x+1) = 1 + \sum_{i=1}^{8} A_i x^i, \quad \ldots\ldots\ldots\ldots\ldots\ldots \quad (5.23)$$

where $A_1 = -0.577191652$, $A_2 = 0.988205891$, $A_3 = -0.897056937$, $A_4 = 0.918206857$, $A_5 = -0.756704078$, $A_6 = 0.482199394$, $A_7 = -0.193527818$, and $A_8 = 0.035868343$ for $0 \leqq x \leqq 1$. The recurrence formula, $\Gamma(x+1) = x\Gamma(x)$, is used for $x > 1$ and $x < 1$; furthermore, $\Gamma(1) = 1$.

The equations for calculating z_i and M_i are summarized in a short FORTRAN program GAMSPL found in Appendix A. In this simple program, the boundary molecular weights are chosen arbitrarily at increments of 14 for the first 19 fractions, starting with η as the first lower boundary. The last fraction is calculated by setting the upper molecular-weight boundary equal to 10,000. **Table 5.4** gives three sample outputs from GAMSPL for $\alpha = 0.5$, 1, and 2 with $\eta = 90$ and $M_{C_{7+}} = 200$ held constant. **Fig. 5.9** plots the results as log z_i vs. M_i. The amount and molecular weight of the C_{26+} fraction varies for each value of α.

The gamma distribution can be fit to experimental molar-distribution data by use of a nonlinear least-squares algorithm to determine α, η, and β. Experimental TBP data are required, including weight fraction and molecular weight for at least five C_{7+} fractions (use of more than 10 fractions is recommended to ensure a unique fit of model parameters). The sum-of-squares function can be defined as

$$F(\alpha, \eta, \beta) = \sum_{i=1}^{N-1} (\Delta_{Mi})^2, \quad \ldots\ldots\ldots\ldots\ldots\ldots \quad (5.24)$$

$$\text{where } \Delta_{Mi} = \frac{(M_i)_{\text{mod}} - (M_i)_{\text{exp}}}{(M_i)_{\text{exp}}}. \quad \ldots\ldots\ldots\ldots\ldots \quad (5.25)$$

Subscripts mod and exp = model and experimental, respectively. This sum-of-squares function weights the lower molecular weights more than higher molecular weights, in accordance with the expected accuracy for measurement of molecular weight. Also, the sum-of-squares function does not include the last molecular weight because this molecular weight may be inaccurate or backcalculated to match the measured average C_{7+} molecular weight. If the last fraction is not included, the model average molecular weight, $(M_{C_{7+}})_{\text{mod}} = \eta + \alpha\beta$, can be compared with the experimental value as an independent check of the fit.

A simple graphical procedure can be used to fit parameters α and η if experimental $M_{C_{7+}}$ is fixed and used to define β. **Fig. 5.10** shows a plot of cumulative weight fraction,

$$Q_{wi} = \sum_{j=1}^{i} w_i, \quad \ldots\ldots\ldots\ldots\ldots\ldots\ldots\ldots \quad (5.26)$$

vs. the cumulative dimensionless molecular-weight variable,

$$Q^*_{Mi} = \frac{Q_{Mi} - \eta}{M_{C_{7+}} - \eta}. \quad \ldots\ldots\ldots\ldots\ldots\ldots\ldots \quad (5.27)$$

Table 5.5 and the following outline describe the procedure for determining model parameters with Fig. 5.10 and TBP data.

1. Tabulate measured mole fractions z_i and molecular weights M_i for each fraction.
2. Calculate experimental weight fractions, $w_i = (z_i M_i) \div (z_{C_{7+}} M_{C_{7+}})$, if they are not reported.
3. Normalize weight fractions and calculate cumulative normalized weight fraction Q_{wi}.
4. Calculate cumulative molecular weight Q_{Mi} from Eq. 5.3.
5. Assume several values of η (e.g., from 75 to 100) and calculate Q^*_{Mi} for each value of the estimated η.
6. For each estimate of η, plot Q^*_{Mi} vs. Q_{wi} on a copy of Fig. 5.10 and choose the curve that fits one of the model curves best. Read the value of α from Fig. 5.10.
7. Calculate molecular weights and mole fractions of Fractions i using the best-fit curve in Fig. 5.10. Enter the curve at measured values of Q_{wi}, read Q^*_{Mi}, and calculate M_i from

$$M_i = \eta + \left(M_{C_{7+}} - \eta\right) \frac{Q_{wi} - Q_{wi-1}}{\left[\left(Q_{wi}/Q^*_{Mi}\right) - \left(Q_{wi-1}/Q^*_{Mi-1}\right)\right]}. \quad \ldots\ldots\ldots\ldots\ldots \quad (5.28)$$

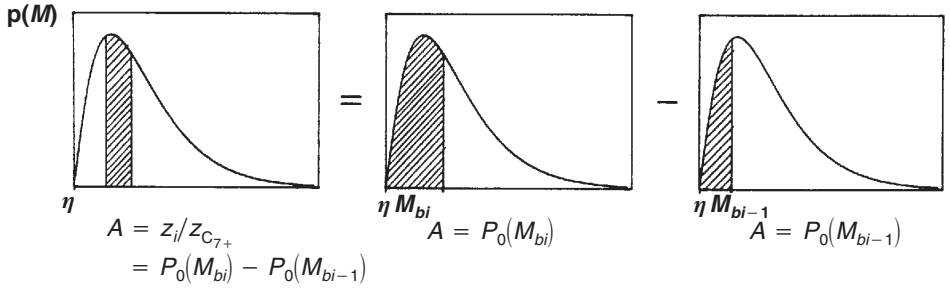

Fig. 5.8—Schematic showing the graphical interpretation of areas under the gamma density function p(*M*) that are proportional to normalized mole fraction; *A* = area.

TABLE 5.4—RESULTS OF GAMSPL PROGRAM FOR THREE DATA SETS WITH DIFFERENT GAMMA-DISTRIBUTION PARAMETER α

	$\alpha = 0.5$		$\alpha = 1.0$		$\alpha = 2.0$	
Fraction Number	Mole Fraction	Molecular Weight	Mole Fraction	Molecular Weight	Mole Fraction	Molecular Weight
1	0.2787233	94.588	0.1195065	96.852	0.0273900	99.132
2	0.1073842	110.525	0.1052247	110.852	0.0655834	111.490
3	0.0772607	124.690	0.0926497	124.852	0.0852269	125.172
4	0.0610991	138.758	0.0815774	138.852	0.0927292	139.038
5	0.0505020	152.796	0.0718284	152.852	0.0925552	152.963
6	0.0428377	166.819	0.0632444	166.852	0.0877762	166.916
7	0.0369618	180.836	0.0556863	180.852	0.0804707	180.883
8	0.0322804	194.848	0.0490314	194.852	0.0720157	194.859
9	0.0284480	208.857	0.0431719	208.852	0.0632969	208.841
10	0.0252470	222.864	0.0380125	222.852	0.0548597	222.826
11	0.0225321	236.870	0.0334698	236.852	0.0470180	236.814
12	0.0202013	250.875	0.0294699	250.852	0.0399302	250.805
13	0.0181808	264.879	0.0259481	264.852	0.0336535	264.797
14	0.0164152	278.883	0.0228471	278.852	0.0281813	278.790
15	0.0148619	292.886	0.0201167	292.852	0.0234690	292.784
16	0.0134879	306.888	0.0177127	306.852	0.0194514	306.778
17	0.0122665	320.890	0.0155959	320.852	0.0160543	320.774
18	0.0111762	334.892	0.0137321	334.852	0.0132017	334.770
19	0.0101996	348.894	0.0120910	348.852	0.0108204	348.766
20	0.1199341	539.651	0.0890834	466.000	0.0463166	420.424
Total	1.0000000		1.0000000		1.0000000	
Average		200		200		200

For all three cases $\eta = 90$ and $M_{C_{7+}} = 200$.

Mole fractions z_i are given by

$$z_i = z_{C7+}\left(\frac{Q_{wi}}{Q^*_{Mi}} - \frac{Q_{wi-1}}{Q^*_{Mi-1}}\right). \quad \ldots\ldots\ldots\ldots\ldots\ldots \quad (5.29)$$

For computer applications, Q_{wi} and Q^*_{Mi} can be calculated exactly from Eqs. 5.16 through 5.23 with little extra effort.

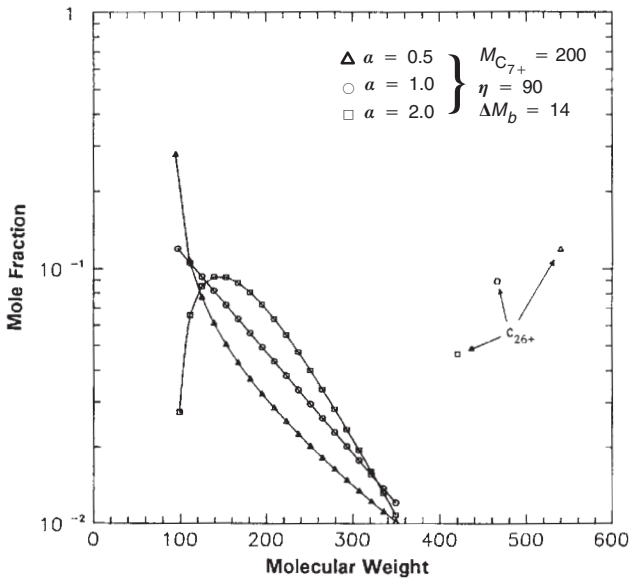

Fig. 5.9—Three example molar distributions for an oil sample with $M_{C_{7+}} = 200$ and $\eta = 90$, calculated with the GAMSPL program (Table A-4) in Table 5.4.

Fig. 5.11 shows a $Q^*_{Mi} - Q_{wi}$ match for the Hoffman *et al.*[29] oil with $\eta = 70$, 72.5, 75, and 80 and indicates that a best fit is achieved for $\eta = 72.5$ and $\alpha = 2.5$ (see **Fig. 5.12**).

Although the gamma-distribution model has the flexibility of treating reservoir fluids from light condensates to bitumen, most reservoir fluids can be characterized with an exponential molar distribution ($\alpha = 1$) without adversely affecting the quality of EOS pre-

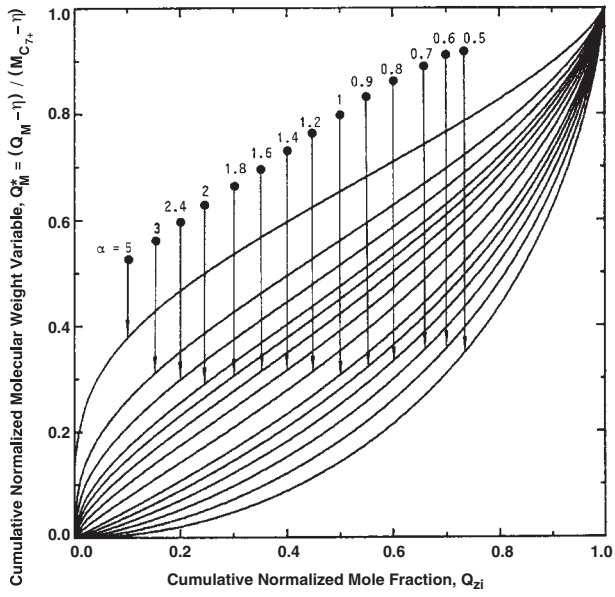

Fig. 5.10—Cumulative-distribution type curve for fitting experimental TBP data to the gamma-distribution model. Parameters α and η are determined with $M_{C_{7+}}$ held constant.

TABLE 5.5—CALCULATION OF CUMULATIVE WEIGHT FRACTION AND CUMULATIVE MOLECULAR WEIGHT VARIABLE FOR HOFFMAN *et al.*[29] OIL

Component								Q^*_{Mi}				
i	z_i	Σz_i	M_i	z_iM_i	Σz_iM_i	Q_{wi}	Q_{Mi}	$\eta=70$	$\eta=72.5$	$\eta=75$	$\eta=80$	$\eta=85$
7	0.0263	0.0263	99	2.604	2.604	0.036	99.0	0.225	0.210	0.194	0.160	0.123
8	0.0234	0.0497	110	2.574	5.178	0.071	104.2	0.266	0.251	0.236	0.204	0.169
9	0.0235	0.0732	121	2.844	8.021	0.110	109.6	0.308	0.294	0.280	0.249	0.216
10	0.0224	0.0956	132	2.957	10.978	0.150	114.8	0.348	0.335	0.322	0.293	0.262
11	0.0241	0.1197	145	3.497	14.475	0.198	120.9	0.396	0.384	0.371	0.345	0.316
12	0.0246	0.1443	158	3.882	18.357	0.251	127.2	0.445	0.434	0.422	0.398	0.371
13	0.0266	0.1709	172	4.570	22.928	0.313	134.2	0.499	0.489	0.478	0.457	0.433
14	0.0326	0.2035	186	6.067	28.995	0.396	142.5	0.563	0.555	0.546	0.526	0.506
15	0.0363	0.2398	203	7.371	36.366	0.497	151.7	0.634	0.627	0.620	0.604	0.586
16	0.0229	0.2627	222	5.093	41.458	0.566	157.8	0.682	0.676	0.669	0.655	0.640
17	0.0171	0.2799	238	4.079	45.538	0.622	162.7	0.720	0.715	0.709	0.697	0.683
18	0.0143	0.2941	252	3.596	49.134	0.671	167.0	0.754	0.749	0.744	0.733	0.722
19	0.0130	0.3072	266	3.466	52.600	0.719	171.2	0.787	0.782	0.778	0.769	0.758
20	0.0108	0.3180	279	3.008	55.607	0.760	174.9	0.815	0.811	0.808	0.799	0.791
21	0.0087	0.3267	290	2.526	58.133	0.794	178.0	0.839	0.836	0.832	0.825	0.818
22	0.0072	0.3338	301	2.152	60.285	0.824	180.6	0.859	0.857	0.854	0.847	0.841
23	0.0058	0.3396	315	1.811	62.097	0.848	182.9	0.877	0.875	0.872	0.867	0.861
24	0.0048	0.3444	329	1.582	63.679	0.870	184.9	0.893	0.891	0.889	0.884	0.879
25	0.0039	0.3483	343	1.351	65.031	0.888	186.7	0.907	0.905	0.903	0.899	0.894
26	0.0034	0.3517	357	1.196	66.227	0.905	188.3	0.919	0.918	0.916	0.913	0.909
27	0.0028	0.3545	371	1.039	67.265	0.919	189.8	0.931	0.929	0.928	0.925	0.921
28	0.0025	0.3570	385	0.963	68.228	0.932	191.1	0.941	0.940	0.939	0.936	0.933
29	0.0023	0.3593	399	0.926	69.154	0.945	192.5	0.952	0.951	0.950	0.948	0.945
30	0.0091	0.3684	444	4.049	73.203	1.000	198.7	1.000	1.000	1.000	1.000	1.000
Total	0.3684		198.7	73.203								

dictions. Whitson *et al.*[27] proposed perhaps the most useful application of the gamma-distribution model. With Gaussian quadrature, their method allows multiple reservoir-fluid samples from a common reservoir to be treated simultaneously with a single fluid characterization. Each fluid sample can have different C_{7+} properties when the split is made so that each split fraction has the same molecular weight (and other properties, such as γ, T_b, T_c, p_c, and ω), while the mole fractions are different for each fluid sample. Example applications include the characterization of a gas cap and underlying reservoir oil and a reservoir with compositional gradient.

The following outlines the procedure for applying Gaussian quadrature to the gamma-distribution function.

1. Determine the number of C_{7+} fractions, N, and obtain the quadrature values X_i and W_i from **Table 5.6** (values are given for $N=3$ and $N=5$).

2. Specify η and α. When TBP data are not available to determine these parameters, recommended values are $\eta=90$ and $\alpha=1$.

3. Specify the heaviest molecular weight of fraction N (recommended value is $M_N = 2.5M_{C_{7+}}$). Calculate a modified β^* term, $\beta^* = (M_N - \eta)/X_N$.

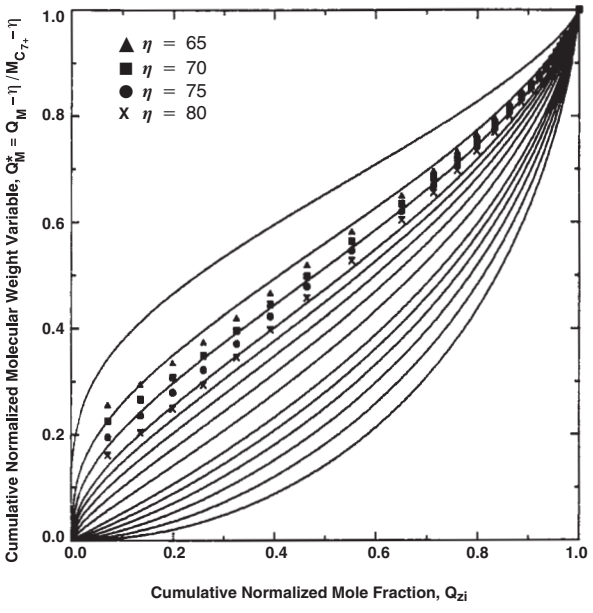

Fig. 5.11—Graphical fit of the Hoffman *et al.*[29] oil molar distribution by use of the cumulative-distribution type curve. Best-fit model parameters are $\alpha=2.5$ and $\eta=72.5$.

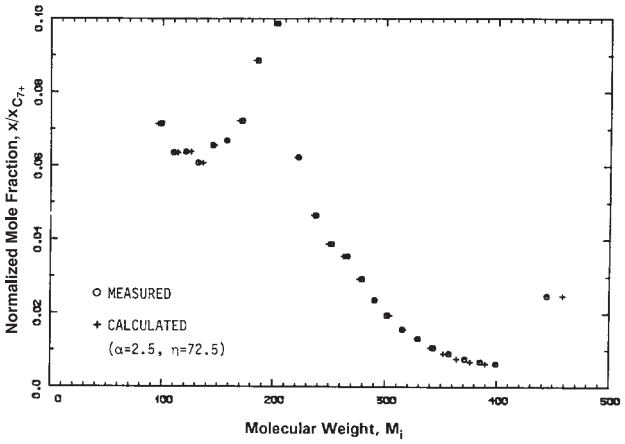

Fig. 5.12—Calculated normalized mole fraction vs. molecular weight of fractions for the Hoffman *et al.*[29] oil based on the best fit in Fig. 5.11 with $\alpha=2.5$ and $\eta=72.5$.

TABLE 5.6—GAUSSIAN QUADRATURE FUNCTION VARIABLES, *X*, AND WEIGHT FACTORS, *W*

	X	*W*
	Three Quadrature Points (plus fractions)	
1	0.415 774 556 783	$7.110\,930\,099\,29\times10^{-1}$
2	2.294 280 360 279	$2.785\,177\,335\,69\times10^{-1}$
3	6.289 945 082 937	$1.038\,925\,650\,16\times10^{-2}$
	Five Quadrature Points (plus fractions)	
1	0.263 560 319 718	$5.217\,556\,105\,83\times10^{-1}$
2	1.413 403 059 107	$3.986\,668\,110\,83\times10^{-1}$
3	3.596 425 771 041	$7.594\,244\,968\,17\times10^{-2}$
4	7.085 810 005 859	$3.611\,758\,679\,92\times10^{-3}$
5	12.640 800 844 276	$2.336\,997\,238\,58\times10^{-5}$

Quadrature function values and weight factors can be found for other quadrature numbers in mathematical handbooks.[30]

4. Calculate the parameter δ.

$$\delta = \exp\left(\frac{\alpha\beta^*}{M_{C_{7+}} - \eta} - 1\right). \quad \text{..... (5.30)}$$

5. Calculate the C_{7+} mole fraction z_i and M_i for each fraction.

$$z_i = z_{C_{7+}}\left[W_i\, f(X_i)\right],$$

$$M_i = \eta + \beta^* X_i,$$

$$\text{and } f(X) = \frac{(X)^{\alpha-1}}{\Gamma(\alpha)}\frac{(1 + \ln\delta)^{\alpha}}{\delta^{X}}. \quad \text{..... (5.31)}$$

6. Check whether the calculated $M_{C_{7+}}$ from Eq. 5.12 equals the measured value used in Step 4 to define δ. Because Gaussian quadrature is only approximate, the calculated $M_{C_{7+}}$ may be slightly in error. This can be corrected by (slightly) modifying the value of δ, and repeating Steps 5 and 6 until a satisfactory match is achieved.

When characterizing multiple samples simultaneously, the values of M_N, η, and β^* must be the same for all samples. Individual sample values of $M_{C_{7+}}$ and α can, however, be different. The result of this characterization is one set of molecular weights for the C_{7+} fractions, while each sample has different mole fractions z_i (so that their average molecular weights $M_{C_{7+}}$ are honored).

Specific gravities for the C_{7+} fractions can be calculated with one of the correlations given in Sec. 5.4 (e.g., Eq. 5.44), where the characterization factor (e.g., F_c) must be the same for all mixtures. The specific gravities, $\gamma_{C_{7+}}$, of each sample will not be exactly reproduced with this procedure (calculated with Eq. 5.37), but the average characterization factor can be chosen so that the differences are very small ($\gamma \pm 0.0005$). Having defined M_i and γ_i for the C_{7+} fractions, a complete fluid characterization can be determined with correlations in Sec. 5.5.

5.4 Inspection-Properties Estimation

5.4.1 Generalized Properties. The molecular weight, specific gravity, and boiling point of C_{7+} fractions must be estimated in the absence of experimental TBP data. This situation arises when simulated distillation is used or when no experimental analysis of C_{7+} is available and a synthetic split must be made by use of a molar-distribution model. For either situation, inspection data from TBP analysis of a sample from the same field would be the most reliable source of M, γ, and T_b for each C_{7+} fraction. The next-best source would be measured TBP data from a field producing similar oil or condensate from the same geological formation. Generalized properties from a producing region, such as the North Sea, have been proposed.[31]

Katz and Firoozabadi[6] suggest a generalized set of SCN properties for petroleum fractions C_6 through C_{45}. Table 5.2 gives an extended version of the Katz-Firoozabadi property table. Molecular weights can be used to convert weight fractions, w_i, from simulated distillation to mole fractions,

$$z_i = \frac{w_i/M_i}{\sum_{j=7}^{N} w_j/M_j}. \quad \text{..... (5.32)}$$

However, the molecular weight of the heaviest fraction, C_N, is not known. From a mass balance, M_N is given by

$$M_N = \frac{w_N}{\left(w_{C_{7+}}/M_{C_{7+}}\right) - \sum_{i=7}^{N-1}(w_i/M_i)}, \quad \text{..... (5.33)}$$

where M_i for $i = 7,\ldots,N-1$ are taken from Table 5.2. Unfortunately, the calculated molecular weight M_N is often unrealistic because of measurement errors in $M_{C_{7+}}$ or in the chromatographic analysis and because generalized molecular weights are only approximate. Both w_N and $M_{C_{7+}}$ can be adjusted to give a "reasonable" M_N, but caution is required to avoid nonphysical adjustments. The same problem is inherent with backcalculating M_N with any set of generalized molecular weights used for SCN Fractions 7 to $N-1$ (e.g., paraffin values).

During the remainder of this section, molecular weights and mole fractions are assumed to be known for C_{7+} fractions, either from chromatographic analysis or from a synthetic split. The generalized properties for specific gravity and boiling point can be assigned to SCN fractions, but the heaviest specific gravity must be backcalculated to match the measured C_{7+} specific gravity. The calculated γ_N also may be unrealistic, requiring some adjustment to generalized specific gravities. Finally, the boiling point of the heaviest fraction must be estimated. T_{bN} can be estimated from a correlation relating boiling point to specific gravity and molecular weight.

5.4.2 Characterization Factors. Inspection properties M, γ, and T_b reflect the chemical makeup of petroleum fractions. Some methods for estimating specific gravity and boiling point assume that a particular characterization factor is constant for all C_{7+} fractions. These methods are only approximate but are widely used.

Watson or Universal Oil Products (UOP) Characterization Factor. The Watson or UOP factor, K_w, is based on normal boiling point, T_b, in °R and specific gravity, γ.[32,33]

$$K_w \equiv \frac{T_b^{1/3}}{\gamma}. \quad \text{..... (5.34)}$$

K_w varies roughly from 8.5 to 13.5. For paraffinic compounds, $K_w = 12.5$ to 13.5; for naphthenic compounds, $K_w = 11.0$ to 12.5; and for aromatic compounds, $K_w = 8.5$ to 11.0. Some overlap in K_w exists among these three families of hydrocarbons, and a combination of paraffins and aromatics will obviously "appear" naphthenic. However, the utility of this and other characterization factors is that they give a qualitative measure of the composition of a petroleum fraction. The Watson characterization factor has been found to be useful for approximate characterization and is widely used as a parameter for correlating petroleum-fraction properties, such as molecular weight, viscosity, vapor pressure, and critical properties.

An approximate relation[2] for the Watson factor, based on molecular weight and specific gravity, is

$$K_w \approx 4.5579\, M^{0.15178}\, \gamma^{-0.84573}. \quad \text{..... (5.35)}$$

This relation is derived from the Riazi-Daubert[14] correlation for molecular weight and is generally valid for petroleum fractions with normal boiling points ranging from 560 to 1,310°R (C_7 through C_{30}). Experience has shown, however, that Eq. 5.35 is not very accurate for fractions heavier than C_{20}.

K_w calculated with $M_{C_{7+}}$ and $\gamma_{C_{7+}}$ in Eq. 5.35 is often constant for a given field. **Figs. 5.13A and 5.13B**[7] plot molecular weight vs. specific gravity for C_{7+} fractions from two North Sea fields. Data for the gas condensate in Fig. 5.13A indicate an average $K_{wC_{7+}} = 11.99 \pm 0.01$ for a range of molecular weights from 135 to 150. The volatile oil shown in Fig. 5.13B has an average $K_{wC_{7+}} = 11.90 \pm 0.01$ for a range of molecular weights from 220 to

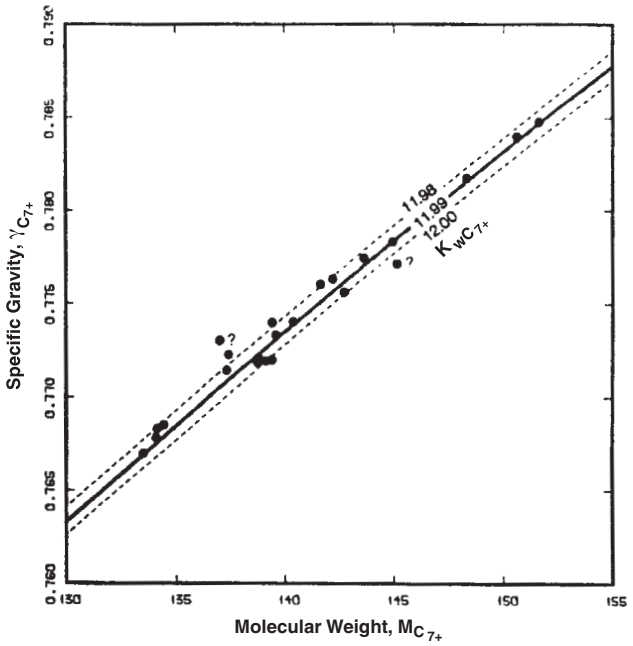

Fig. 5.13A—Specific gravity vs. molecular weight for C_{7+} fractions for a North Sea Gas-Condensate Field 2 (after Austad *et al.*[7]).

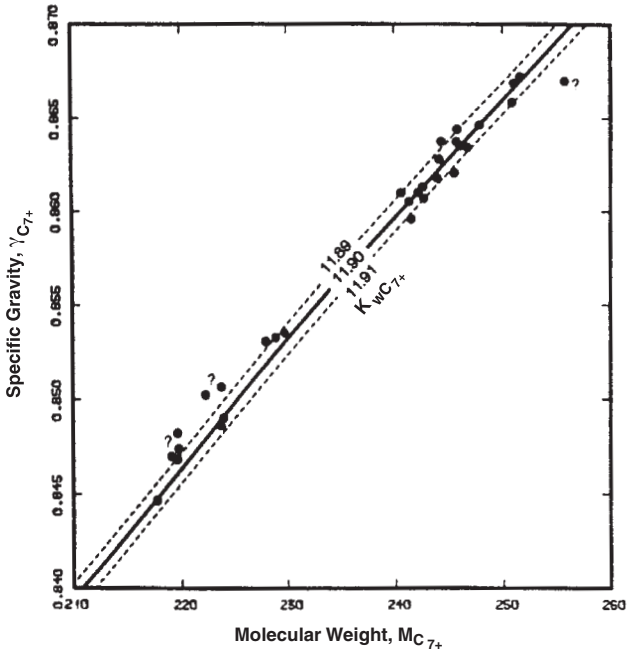

Fig. 5.13B—Specific gravity vs. molecular weight for C_{7+} fractions for a North Sea Volatile-Oil Field 3B(after Austad *et al.*[7]).

255. The high degree of correlation for these two fields suggests accurate molecular-weight measurements by the laboratory. In general, the spread in $K_{wC_{7+}}$ values will exceed ± 0.01 when measurements are performed by a commercial laboratory.

When the characterization factor for a field can be determined, Eq. 5.35 is useful for checking the consistency of C_{7+} molecular-weight and specific-gravity measurements. Significant deviation in $K_{wC_{7+}}$, such as ± 0.03 for the North Sea fields above, indicates possible error in the measured data. Because molecular weight is more prone to error than determination of specific gravity, an anomalous $K_{wC_{7+}}$ usually indicates an erroneous molecular-weight measurement. For the gas condensate in Fig. 5.13A, a C_{7+} sample with specific gravity of 0.775 would be expected to have a molecular weight of $\approx$141 (for $K_{wC_{7+}} = 11.99$). If the measured value was 135, the Watson characterization factor would be 11.90, which is significantly lower than the field average of 11.99. In this case, the C_{7+} molecular weight should be redetermined.

Eq. 5.35 can also be used to calculate specific gravity of C_{7+} fractions determined by simulated distillation or a synthetic split (i.e., when only mole fractions and molecular weights are known). Assuming a constant K_w for each fraction, specific gravity, γ_i, can be calculated from

$$\gamma_i = 6.0108\, M_i^{0.17947}\, K_w^{-1.18241}. \quad \ldots\ldots\ldots\ldots\ldots\ldots \quad (5.36)$$

K_w must be chosen so that experimentally measured C_{7+} specific gravity, $(\gamma_{C_{7+}})_{exp}$, is calculated correctly.

$$\left(\gamma_{C_{7+}}\right)_{exp} = \frac{z_{C_{7+}} M_{C_{7+}}}{\sum_{i=1}^{N} \left(z_i M_i / \gamma_i\right)}. \quad \ldots\ldots\ldots\ldots\ldots\ldots \quad (5.37)$$

The Watson factor satisfying Eq. 5.37 is given by

$$K_w = \left[\frac{0.16637 \gamma_{C_{7+}} A_0}{z_{C_{7+}} M_{C_{7+}}}\right]^{-0.84573}, \quad \ldots\ldots\ldots\ldots\ldots\ldots \quad (5.38)$$

where $A_0 = \sum_{i=1}^{N} z_i M_i^{0.82053}$. $\quad \ldots\ldots\ldots\ldots\ldots\ldots \quad (5.39)$

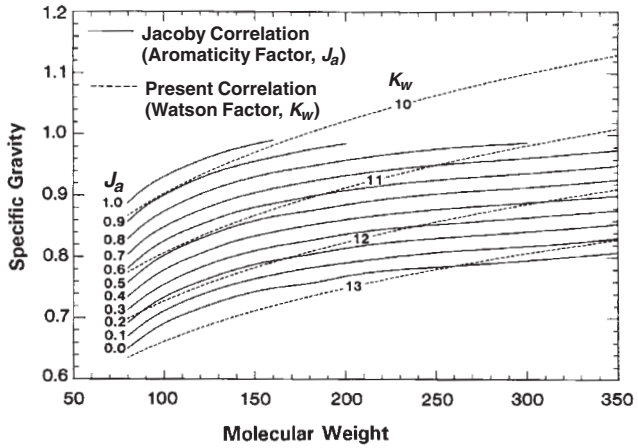

Fig. 5.14—Specific gravity vs. molecular weight for constant values of the Jacoby aromaticity factor (solid lines) and the Watson characterization factor (dashed lines). After Whitson.[25]

Boiling points, T_{bi}, can be estimated from Eq. 5.36.

$$T_{bi} = (K_w \gamma_i)^3. \quad \ldots\ldots\ldots\ldots\ldots\ldots \quad (5.40)$$

Unfortunately, Eqs. 5.36 through 5.40 overpredict γ and T_b at molecular weights greater than $\approx$250 (an original limitation of the Riazi-Daubert[14] molecular-weight correlation).

Jacoby Aromaticity Factor. The Jacoby aromaticity factor, J_a, is an alternative characterization factor for describing the relative composition of petroleum fractions.[34] **Fig. 5.14**[2] shows the original Jacoby relation between specific gravity and molecular weight for several values of J_a. The behavior of specific gravity as a function of molecular weight is similar for the Jacoby factor and the relation for a constant K_w. However, specific gravity calculated with the Jacoby method increases more rapidly at low molecular weights, flattening at high molecular weights (a more physically consistent behavior). A relation for the Jacoby factor is

$$J_a = \frac{\gamma - 0.8468 + (15.8/M)}{0.2456 - (1.77/M)} \quad \ldots\ldots\ldots\ldots\ldots\ldots \quad (5.41)$$

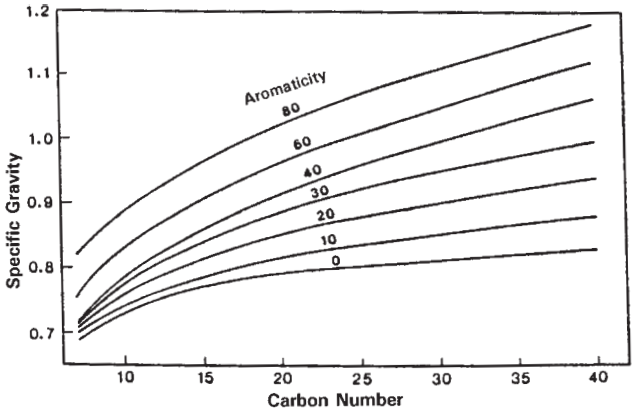

Fig. 5.15—Specific gravity vs. carbon number for constant values of the Yarborough aromaticity factor (after Yarborough[1]).

or, in terms of specific gravity,

$$\gamma = 0.8468 - \frac{15.8}{M} + J_a\left(0.2456 - \frac{1.77}{M}\right). \quad \ldots\ldots (5.42)$$

The first two terms in Eq. 5.42 (i.e., when $J_a = 0$) express the relation between specific gravity and molecular weight for normal paraffins.

The Jacoby factor can also be used to estimate fraction specific gravities when mole fractions and molecular weights are available from simulated distillation or a synthetic split. The Jacoby factor satisfying measured C_{7+} specific gravity (Eq. 5.37) must be calculated by trial and error. We have found that this relation is particularly accurate for gas-condensate systems.[27]

Yarborough Aromaticity Factor. Yarborough[1] modified the Jacoby aromaticity factor specifically for estimating specific gravities when mole fractions and molecular weights are known. Yarborough tries to improve the original Jacoby relation by reflecting the changing character of fractions up to C_{13} better and by representing the larger naphthenic content of heavier fractions better. **Fig. 5.15** shows how the Yarborough aromaticity factor, Y_a, is related to specific gravity and carbon number. A simple relation representing Y_a is not available; however, Whitson[26] has fit the seven aromaticity curves originally presented by Yarborough using the equation

$$\gamma_i = \exp\left[A_0 + A_1 i^{-1} + A_2 i + A_3 \ln(i)\right], \quad \ldots\ldots (5.43)$$

where i = carbon number. **Table 5.7** gives the constants for Eq. 5.43. The aromaticity factor required to satisfy measured C_{7+} specific gravity (Eq. 5.37) is determined by trial and error. Linear interpolation of specific gravity should be used to calculate specific gravity for a Y_a value falling between two values of Y_a in Table 5.7.

Søreide[35] Correlations. Søreide developed an accurate specific-gravity correlation based on the analysis of 843 TBP fractions from 68 reservoir C_{7+} samples.

$$\gamma_i = 0.2855 + C_f(M_i - 66)^{0.13}. \quad \ldots\ldots (5.44)$$

C_f typically has a value between 0.27 and 0.31 and is determined for a specific C_{7+} sample by satisfying Eq. 5.37.

5.4.3 Boiling-Point Estimation. Boiling point can be estimated from molecular weight and specific gravity with one of several correlations. Søreide also developed a boiling-point correlation based on 843 TBP fractions from 68 reservoir C_{7+} samples,

$$T_b = 1928.3 - \left(1.695 \times 10^5\right) M^{-0.03522}\gamma^{3.266} \times \exp\left[-\left(4.922 \times 10^{-3}\right)M - 4.7685\gamma + \left(3.462 \times 10^{-3}\right)M\gamma\right], \quad \ldots\ldots (5.45)$$

with T_b in °R.

Table 5.8 gives estimated specific gravities determined with the methods just described for a C_{7+} sample with the exponential split given in Table 5.4 ($\alpha = 1$, $\eta = 90$, $M_{C_{7+}} = 200$) and $\gamma_{C_{7+}} = 0.832$.

The following equations also relate molecular weight to boiling point and specific gravity; any of these correlations can be solved for boiling point in terms of M and γ. We recommend, however, the Søreide correlation for estimating T_b from M and γ.

Kesler and Lee.[12]

$$M = \left[-12,272.6 + 9,486.4\gamma + (4.6523 - 3.3287\gamma)T_b\right] + \left\{\left(1 - 0.77084\gamma - 0.02058\gamma^2\right) \times \left[\left(1.3437 - 720.79T_b^{-1}\right) \times 10^7\right]T_b^{-1}\right\} + \left\{\left(1 - 0.80882\gamma + 0.02226\gamma^2\right) \times \left[\left(1.8828 - 181.98T_b^{-1}\right) \times 10^{12}\right]T_b^{-3}\right\}. \quad \ldots\ldots (5.46)$$

Riazi and Daubert.[14]

$$M = \left(4.5673 \times 10^{-5}\right)T_b^{2.1962}\gamma^{-1.0164}. \quad \ldots\ldots (5.47)$$

American Petroleum Inst. (API).[36]

$$M = \left(2.0438 \times 10^2\right)T_b^{0.118}\gamma^{1.88}\exp(0.00218T_b - 3.07\gamma). \quad \ldots\ldots (5.48)$$

Rao and Bardon.[37]

$$\ln M = (1.27 + 0.071K_w)\ln\left(\frac{1.8T_b}{22.31 + 1.68K_w}\right). \quad \ldots\ldots (5.49)$$

Riazi and Daubert.[18]

$$M = 581.96T_b^{0.97476}\gamma^{6.51274}\exp\left[\left(5.43076 \times 10^{-3}\right)T_b - 9.53384\gamma + \left(1.11056 \times 10^{-3}\right)T_b\gamma\right]. \quad \ldots\ldots (5.50)$$

TABLE 5.7—COEFFICIENTS FOR YARBOROUGH AROMATICITY FACTOR CORRELATION[1,26]

Y_a	A_0	A_1	A_2	A_2
0.0	-7.43855×10^{-2}	-1.72341	1.38058×10^{-3}	-3.34169×10^{-2}
0.1	-4.25800×10^{-1}	-7.00017×10^{-1}	-3.30947×10^{-5}	8.65465×10^{-2}
0.2	-4.47553×10^{-1}	-7.65111×10^{-1}	1.77982×10^{-4}	1.07746×10^{-1}
0.3	-4.39105×10^{-1}	-9.44068×10^{-1}	4.93708×10^{-4}	1.19267×10^{-1}
0.4	-2.73719×10^{-1}	-1.39960	3.80564×10^{-3}	5.92005×10^{-2}
0.6	-7.39412×10^{-3}	-1.97063	5.87273×10^{-3}	-1.67141×10^{-2}
0.8	-3.17618×10^{-1}	-7.78432×10^{-1}	2.58616×10^{-3}	1.08382×10^{-3}

TABLE 5.8—COMPARISON OF SPECIFIC GRAVITIES WITH CORRELATIONS BY USE OF DIFFERENT CHARACTERIZATION FACTORS

			γ_i for Different Correlations With Constant Characterization Factor Chosen To Match $\gamma_{C_{7+}} = 0.832$			
Fraction	z_i	M_i	$K_w = 12.080$	$J_a = 0.2395$	$Y_a = 0.2794$	$C_f = 0.2864$
1	0.1195	96.8	0.7177	0.7472	0.7051	0.7327
2	0.1052	110.8	0.7353	0.7684	0.7286	0.7550
3	0.0926	124.8	0.7511	0.7849	0.7486	0.7719
4	0.0816	138.8	0.7656	0.7981	0.7660	0.7856
5	0.0718	152.8	0.7789	0.8088	0.7813	0.7972
6	0.0632	166.8	0.7913	0.8178	0.7951	0.8072
7	0.0557	180.8	0.8028	0.8253	0.8075	0.8161
8	0.0490	194.8	0.8136	0.8318	0.8189	0.8241
9	0.0432	208.8	0.8238	0.8374	0.8294	0.8314
10	0.0380	222.8	0.8335	0.8423	0.8391	0.8380
11	0.0335	236.8	0.8426	0.8466	0.8482	0.8442
12	0.0295	250.8	0.8514	0.8505	0.8567	0.8500
13	0.0259	264.8	0.8597	0.8539	0.8646	0.8554
14	0.0228	278.8	0.8677	0.8570	0.8722	0.8604
15	0.0201	292.8	0.8753	0.8598	0.8793	0.8652
16	0.0177	306.8	0.8827	0.8623	0.8861	0.8697
17	0.0156	320.8	0.8898	0.8646	0.8926	0.8740
18	0.0137	334.8	0.8966	0.8668	0.8988	0.8782
19	0.0121	348.8	0.9033	0.8687	0.9048	0.8821
20	0.0891	466.0	0.9514	0.8805	0.9468	0.9096
Total	1.0000	200.0	0.8320	0.8320	0.8320	0.8320

5.5 Critical-Properties Estimation

Thus far, we have discussed how to split the C_{7+} fraction into pseudocomponents described by mole fraction, molecular weight, specific gravity, and boiling point. Now we must consider the problem of assigning critical properties to each pseudocomponent. Critical temperature, T_c; critical pressure, p_c; and acentric factor, ω, of each component in a mixture are required by most cubic EOS's. Critical volume, v_c, is used instead of critical pressure in the Benedict-Webb-Rubin[38] (BWR) EOS, and critical molar volume is used with the LBC viscosity correlation.[24] Critical compressibility factor has been introduced as a parameter in three- and four-constant cubic EOS's.

Critical-property estimation of petroleum fractions has a long history beginning as early as the 1930's; several reviews[22,25,26,39,40] are available. We present the most commonly used correlations and a graphical comparison (**Figs. 5.16 through 5.18**) that is intended to highlight differences between the correlations. Finally, correlations based on perturbation expansion (a concept borrowed from statistical mechanics) are discussed separately.

The units for the remaining equations in this section are T_b in °R, T_{bF} in °F = $T_b - 459.67$, T_c in °R, p_c in psia, and v_c in ft^3/lbm mol. Oil gravity is denoted γ_{API} and is related to specific gravity by $\gamma_{API} = 141.5/\gamma - 131.5$.

5.5.1 Critical Temperature. T_c is perhaps the most reliably correlated critical property for petroleum fractions. The following critical-temperature correlations can be used for petroleum fractions.

***Roess.*[41]** (modified by API[36]).

$$T_c = 645.83 + 1.6667\left[\gamma\left(T_{bF} + 100\right)\right] - \left(0.7127 \times 10^{-3}\right)\left[\gamma\left(T_{bF} + 100\right)\right]^2. \quad \ldots\ldots\ldots\ldots (5.51)$$

***Kesler-Lee.*[12]**

$$T_c = 341.7 + 811\gamma + (0.4244 + 0.1174\gamma)T_b + (0.4669 - 3.2623\gamma) \times 10^5 T_b^{-1}. \quad \ldots\ldots\ldots\ldots (5.52)$$

***Cavett.*[42]**

$$T_c = 768.07121 + 1.7133693T_{bF} - \left(0.10834003 \times 10^{-2}\right)T_{bF}^2 - \left(0.89212579 \times 10^{-2}\right)\gamma_{API}T_{bF} + \left(0.38890584 \times 10^{-6}\right)T_{bF}^3 + \left(0.5309492 \times 10^{-5}\right)\gamma_{API}T_{bF}^2 + \left(0.327116 \times 10^{-7}\right)\gamma_{API}^2 T_{bF}^2. \quad \ldots\ldots\ldots\ldots (5.53)$$

***Riazi-Daubert.*[14]**

$$T_c = 24.27871 T_b^{0.58848}\gamma^{0.3596}. \quad \ldots\ldots\ldots\ldots (5.54)$$

***Nokay.*[43]**

$$T_c = 19.078\, T_b^{0.62164}\gamma^{0.2985}. \quad \ldots\ldots\ldots\ldots (5.55)$$

5.5.2 Critical Pressure. p_c correlations are less reliable than T_c correlations. The following are p_c correlations that can be used for petroleum fractions.

***Kesler-Lee.*[12]**

$$\ln p_c = 8.3634 - \frac{0.0566}{\gamma} - \left[\left(0.24244 + \frac{2.2898}{\gamma} + \frac{0.11857}{\gamma^2}\right) \times 10^{-3}\right]T_b$$

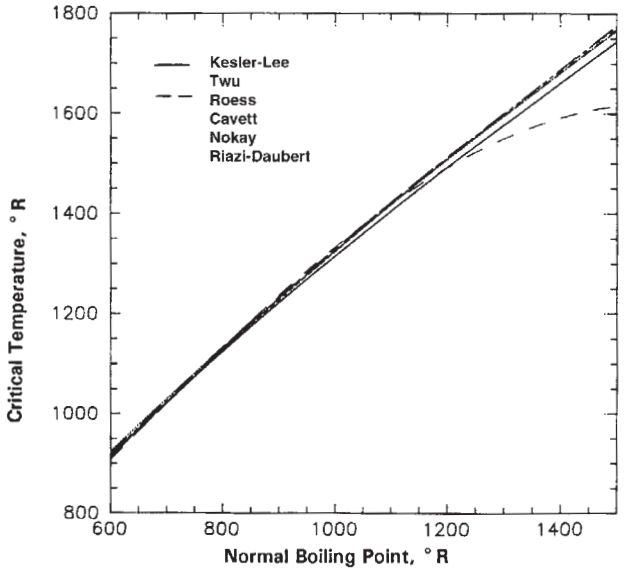

Fig. 5.16—Comparison of critical-temperature correlations for boiling points from 600 to 1,500°R assuming a constant Watson characterization factor of 12.

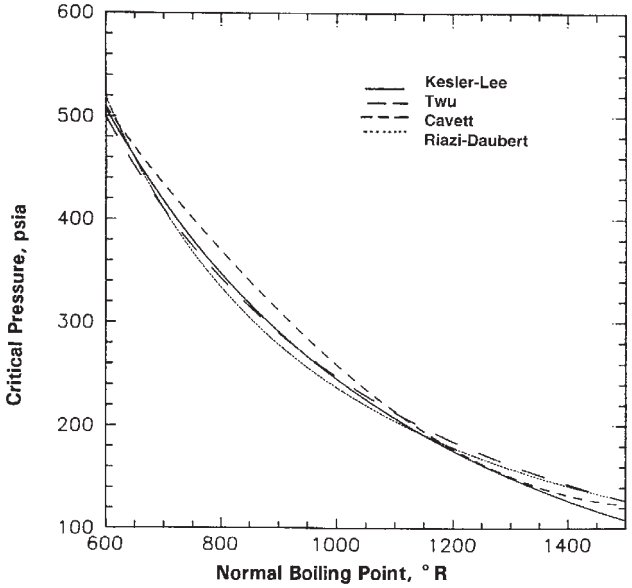

Fig. 5.17—Comparison of critical-pressure correlations for boiling points from 600 to 1,500°R assuming a constant Watson characterization factor of 12.

$$+\left[\left(1.4685+\frac{3.648}{\gamma}+\frac{0.47227}{\gamma^2}\right)\times 10^{-7}\right]T_b^2$$

$$-\left[\left(0.42019+\frac{1.6977}{\gamma^2}\right)\times 10^{-10}\right]T_b^3. \quad \ldots\ldots (5.56)$$

***Cavett.*[42]**

$$\log p_c = 2.8290406 + \left(0.94120109\times 10^{-3}\right)T_{bF} - \left(0.30474749\times 10^{-5}\right)T_{bF}^2 - \left(0.2087611\times 10^{-4}\right)\gamma_{\mathrm{API}}T_{bF} + \left(0.15184103\times 10^{-8}\right)T_{bF}^3 + \left(0.11047899\times 10^{-7}\right)\gamma_{\mathrm{API}}T_{bF}^2 - \left(0.48271599\times 10^{-7}\right)\gamma_{\mathrm{API}}^2T_{bF} + \left(0.13949619\times 10^{-9}\right)\gamma_{\mathrm{API}}^2T_{bF}^2. \quad \ldots\ldots (5.57)$$

***Riazi-Daubert.*[14]**

$$p_c = \left(3.12281\times 10^{9}\right)T_b^{-2.3125}\gamma^{2.3201}. \quad \ldots\ldots (5.58)$$

5.5.3 Acentric Factor. Pitzer *et al.*[44] defined acentric factor as

$$\omega \equiv -\log\left(\frac{p_v^*}{p_c}\right)-1, \quad \ldots\ldots (5.59)$$

where p_v^* = vapor pressure at temperature $T=0.7T_c$ ($T_r=0.7$).

Practically, acentric factor gives a measure of the steepness of the vapor-pressure curve from $T_r=0.7$ to $T_r=1$, where $p_v^*/p_c=0.1$ for $\omega=0$ and $p_v^*/p_c=0.01$ for $\omega=1$. Numerically, $\omega\approx 0.01$ for methane, ≈ 0.25 for C_5, and ≈ 0.5 for C_8 (see Table A.1 for literature values of acentric factor for pure compounds). ω increases to >1.0 for petroleum fractions heavier than approximately C_{25} (see Table 5.2).

The Kesler-Lee[12] acentric factor correlation (for $T_b/T_c>0.8$) is developed specifically for petroleum fractions, whereas the correlation for $T_b/T_c<0.8$ is based on an accurate vapor-pressure correlation for pure compounds. The Edmister[45] correlation is limited to pure hydrocarbons and should not be used for C_{7+} fractions. The three correlations follow.

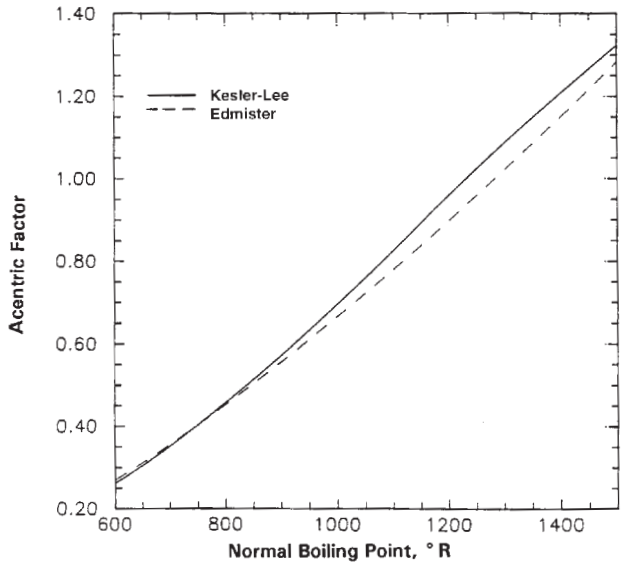

Fig. 5.18—Comparison of acentric factor correlations for boiling points from 600 to 1500°R assuming a constant Watson characterization factor of 12.

***Lee-Kesler.*[13]** ($T_{br}=T_b/T_c<0.8$).

$$\omega = \frac{-\ln(p_c/14.7)+A_1+A_2T_{br}^{-1}+A_3\ln T_{br}+A_4T_{br}^6}{A_5+A_6T_{br}^{-1}+A_7\ln T_{br}+A_8T_{br}^6}, \quad \ldots\ldots (5.60)$$

where $A_1=-5.92714$, $A_2=6.09648$, $A_3=1.28862$, $A_4=-0.169347$, $A_5=15.2518$, $A_6=-15.6875$, $A_7=-13.4721$, and $A_8=0.43577$.

***Kesler-Lee.*[12]** ($T_{br}=T_b/T_c>0.8$).

$$\omega = -7.904+0.1352K_w-0.007465K_w^2+8.359T_{br}+(1.408-0.01063K_w)T_{br}^{-1}. \quad \ldots\ldots (5.61)$$

***Edmister.*[45]**

$$\omega = \frac{3}{7}\frac{\log(p_c/14.7)}{\left[(T_c/T_b)-1\right]}-1. \quad \ldots\ldots (5.62)$$

5.5.4 Critical Volume. The Hall-Yarborough[46] critical-volume correlation is given in terms of molecular weight and specific gravity, whereas the Riazi-Daubert[14] correlation uses normal boiling point and specific gravity.

Hall-Yarborough.[46]

$$v_c = 0.025 M^{1.15} \gamma^{-0.7935}. \quad \ldots\ldots\ldots\ldots\ldots\ldots \quad (5.63)$$

Riazi-Daubert.[14]

$$v_c = \left(7.0434 \times 10^{-7}\right) T_b^{2.3829} \gamma^{-1.683}. \quad \ldots\ldots\ldots\ldots \quad (5.64)$$

Critical compressibility factor, Z_c, is defined as

$$Z_c = \frac{p_c v_c}{R T_c}, \quad \ldots\ldots\ldots\ldots\ldots\ldots\ldots\ldots\ldots \quad (5.65)$$

where R = universal gas constant. Thus, Z_c can be calculated directly from critical pressure, critical volume, and critical temperature. Reid *et al.*[40] and Pitzer *et al.*[44] give an approximate relation for Z_c.

$$Z_c \approx 0.291 - 0.08\omega. \quad \ldots\ldots\ldots\ldots\ldots\ldots\ldots \quad (5.66)$$

Eq. 5.66 is not particularly accurate (grossly overestimating Z_c for heavier compounds) and is used only for approximate calculations.

5.5.5 Correlations Based on Perturbation Expansions. Correlations for critical temperature, critical pressure, critical volume, and molecular weight have been developed for petroleum fractions with a perturbation-expansion model with normal paraffins as the reference system. To calculate critical pressure, for example, critical temperature, critical volume, and specific gravity of a paraffin with the same boiling point as the petroleum fraction must be calculated first. Kesler *et al.*[47] first used the perturbation expansion (with *n*-alkanes as the reference fluid) to develop a suite of critical-property and acentric-factor correlations.

Twu[48] uses the same approach to develop a suite of critical-property correlations. We give his normal-paraffin correlations first, then the correlations for petroleum fractions.

Normal Paraffins (Alkanes).

$$T_{cP} = T_b \Bigg[0.533272 + \left(0.191017 \times 10^{-3}\right) T_b + \left(0.779681 \times 10^{-7}\right) T_b^2 - \left(0.284376 \times 10^{-10}\right) T_b^3 + \frac{(0.959468 \times 10^2)}{(0.01 T_b)^{13}} \Bigg]^{-1}, \quad \ldots\ldots\ldots\ldots\ldots \quad (5.67)$$

$$p_{cP} = (3.83354 + 1.19629\alpha^{0.5} + 34.8888\alpha + 36.1952\alpha^2 + 104.193\alpha^4)^2, \quad \ldots\ldots\ldots\ldots\ldots \quad (5.68)$$

$$v_{cP} = [\, 1 - (0.419869 - 0.505839\alpha - 1.56436\alpha^3 - 9481.7\alpha^{14})]^{-8}, \quad \ldots\ldots\ldots\ldots\ldots\ldots \quad (5.69)$$

$$\gamma_P = 0.843593 - 0.128624\alpha - 3.36159\alpha^3 - 13749.5\alpha^{12}, \quad \ldots\ldots\ldots\ldots\ldots\ldots\ldots \quad (5.70)$$

$$\text{and } T_b = \exp(5.71419 + 2.71579\theta - 0.28659\theta^2 - 39.8544\theta^{-1} - 0.122488\theta^{-2}) - 24.7522\theta + 35.3155\theta^2, \quad \ldots\ldots\ldots\ldots\ldots \quad (5.71)$$

$$\text{where } \alpha = 1 - \frac{T_b}{T_{cP}} \quad \ldots\ldots\ldots\ldots\ldots\ldots\ldots\ldots \quad (5.72)$$

$$\text{and } \theta = \ln M_P. \quad \ldots\ldots\ldots\ldots\ldots\ldots\ldots\ldots\ldots \quad (5.73)$$

Paraffin molecular weight, M_P, is not explicitly a function of T_b, and Eqs. 5.67 through 5.73 must be solved iteratively; an initial guess is given by

$$M_P \approx \frac{T_b}{10.44 - 0.0052 T_b}. \quad \ldots\ldots\ldots\ldots\ldots\ldots \quad (5.74)$$

Twu claims that the normal-paraffin correlations are valid for C_1 through C_{100}, although the properties at higher carbon numbers are only approximate because experimental data for paraffins heavier than approximately C_{20} do not exist. The following relations are used to calculate petroleum-fraction properties.

Critical Temperature.

$$T_c = T_{cP} \left(\frac{1 + 2f_T}{1 - 2f_T} \right)^2,$$

$$f_T = \Delta\gamma_T \left[\frac{-0.362456}{T_b^{0.5}} + \left(0.0398285 - \frac{0.948125}{T_b^{0.5}} \right) \Delta\gamma_T \right],$$

$$\text{and } \Delta\gamma_T = \exp[5(\gamma_P - \gamma)] - 1. \quad \ldots\ldots\ldots\ldots\ldots\ldots \quad (5.75)$$

Critical Volume.

$$v_c = v_{cP} \left(\frac{1 + 2f_v}{1 - 2f_v} \right)^2,$$

$$f_v = \Delta\gamma_v \left[\frac{0.466590}{T_b^{0.5}} + \left(-0.182421 + \frac{3.01721}{T_b^{0.5}} \right) \Delta\gamma_v \right],$$

$$\text{and } \Delta\gamma_v = \exp\left[4\left(\gamma_P^2 - \gamma^2\right)\right] - 1. \quad \ldots\ldots\ldots\ldots\ldots\ldots \quad (5.76)$$

Critical Pressure.

$$p_c = p_{cP} \left(\frac{T_c}{T_{cP}} \right) \left(\frac{V_{cP}}{V_c} \right) \left(\frac{1 + 2f_p}{1 - 2f_p} \right)^2,$$

$$f_p = \Delta\gamma_p \left[\left(2.53262 - \frac{46.1955}{T_b^{0.5}} - 0.00127885 T_b \right) + \left(-11.4277 + \frac{252.14}{T_b^{0.5}} + 0.00230535 T_b \right) \Delta\gamma_p \right],$$

$$\text{and } \Delta\gamma_p = \exp[0.5(\gamma_P - \gamma)] - 1. \quad \ldots\ldots\ldots\ldots\ldots\ldots \quad (5.77)$$

Molecular Weight.

$$\ln M = \ln M_P \left(\frac{1 + 2f_M}{1 - 2f_M} \right)^2,$$

$$f_M = \Delta\gamma_M \left[|x| + \left(-0.0175691 + \frac{0.193168}{T_b^{0.5}} \right) \Delta\gamma_M \right],$$

$$x = 0.012342 - \frac{0.328086}{T_b^{0.5}},$$

$$\text{and } \Delta\gamma_M = \exp[5(\gamma_P - \gamma)]. \quad \ldots\ldots\ldots\ldots\ldots\ldots \quad (5.78)$$

Figs. 5.16 through 5.18 compare the various critical-property correlations for a range of boiling points from 600 to 1,500°R.

5.5.6 Methods Based on an EOS. Fig. 5.19[28] illustrates the important influence that critical properties have on EOS-calculated properties of pure components. Vapor pressure is particularly sensitive to critical temperature. For example, the Riazi-Daubert[19] critical-temperature correlation for toluene overpredicts the experimental value

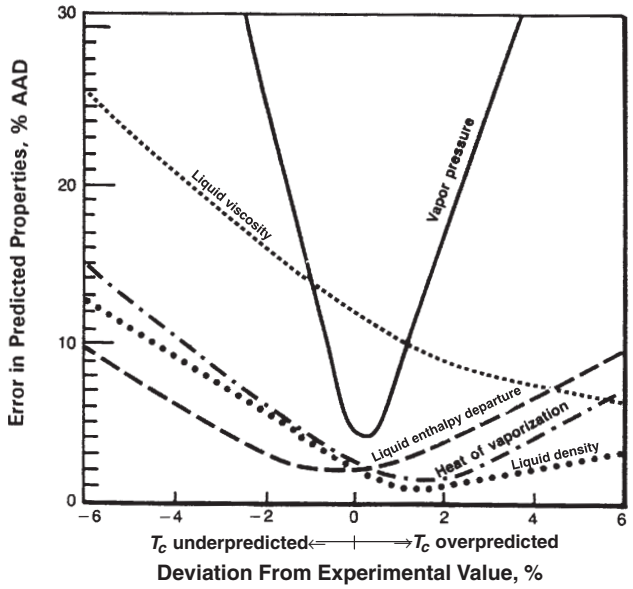

Fig. 5.19—Effect of critical temperature on vapor-pressure prediction of toluene with the PR EOS; AAD = absolute average deviation (after Brulé *et al.*[28]).

by only 1.7%. Even with this slight error in T_c, the average error in vapor pressures predicted by the Peng-Robinson[49] (PR) EOS is 16%. The effect of critical properties and acentric factor on EOS calculations for reservoir-fluid mixtures is summarized by Whitson.[26]

In principle, the EOS used for mixtures should also predict the behavior of individual components found in the mixture. For pure compounds, the vapor pressure is accurately predicted because all EOS's force fit vapor-pressure data. Some EOS's are also fit to saturated-liquid densities at subcritical temperatures. The measured properties of petroleum fractions, boiling point, and specific gravity can also be fit by the EOS, as discussed later.

For each petroleum fraction separately, two of the EOS parameters (T_c; p_c; ω; volume-shift factor, s; or multipliers of EOS constants A and B) can be chosen so that the EOS exactly reproduces experimental boiling point and specific gravity. Because only two inspection properties are available (T_b and γ), only two of the EOS parameters can be determined. Whitson[50] suggests fixing the value of ω with an empirical correlation and adjusting T_c and p_c to match normal boiling point and molar volume (M/γ) at standard conditions. Critical properties satisfying these criteria are given for a wide range of petroleum fractions by the PR EOS and the Soave-Redlich-Kwong (SRK) EOS.[22,23] A better (and recommended) approach for cubic EOS's is to use the volume-shift factor s (see Chap. 4) to match specific gravity or a saturated liquid density and acentric factor to match normal boiling point.

Other methods for forcing the EOS to match boiling point and specific gravity have also been devised. Brulé and Starling[51] proposed a method that uses viscosity as an additional inspection property of the fraction for determining critical properties. This approach proved particularly successful when applied to the BWR EOS for residual-oil supercritical extraction (ROSE).[28]

5.6 Recommended C_{7+} Characterizations

We recommend the following C_{7+} characterization procedure for cubic EOS's.

1. Use the Twu[48] (or Lee-Kesler[12]) critical property correlation for T_c and p_c.
2. Choose the acentric factor to match T_b; alternatively, use the Lee-Kesler[12]/Kesler-Lee[13] correlations.
3. Determine volume-translation coefficients, s_i, to match specific gravities; alternatively, use Peneloux *et al.*'s[52] correlation for the SRK EOS[22,23] or Jhaveri and Youngren's[53] correlation for the PR EOS.[49]

When measured TBP data are not available, a mathematical split should be made with either (1) the gamma distribution (default $\alpha = 1, \eta = 90$) with Gaussian-quadrature or equal-mass fractions or (2) the exponential distribution (Eq. 5.7). Specific gravities should be estimated with the Søreide[35] correlation (Eq. 5.44), choosing C_f to match measured C_{7+} specific gravity (Eq. 5.37). Boiling points should be estimated from the Søreide correlation (Eq. 5.45).

For the PR EOS, we recommend the nonhydrocarbon BIP's given in Chap. 4 and the modified Chueh-Prausnitz[54] equation for C_1 through C_{7+} pairs,

$$k_{ij} = A\left[1 - \left(\frac{2v_{ci}^{1/6}v_{cj}^{1/6}}{v_{ci}^{1/3} + v_{cj}^{1/3}}\right)^{B}\right], \quad \ldots\ldots\ldots\ldots\ldots\ldots (5.79)$$

with $A = 0.18$ and $B = 6$.

5.6.1 SRK-Recommended Characterization. Alternatively, the Pedersen *et al.*[55] characterization procedure can be used with the SRK EOS.

1. Split the plus fraction C_{n+} (preferably $n > 10$) into SCN fractions up to C_{80} using Eqs. 5.7 through 5.11 and $h = -4$.
2. Calculate SCN densities ρ_i ($\gamma_i = \rho_i/0.999$) using the equation $\rho_i = A_0 + A_1 \ln(i)$, where A_0 and A_1 are determined by satisfying the experimental-plus density, ρ_{n+}, and measured (or assumed) density, ρ_{n-1} ($\rho_6 = 0.690$ can be used for C_{7+}).
3. Calculate critical properties of all C_{7+} fractions (distillation cuts from C_7 to C_{n-1} and split SCN fractions from C_n through C_{80}) using the correlations

$$T_c = 163.12\rho + 86.052 \ln M + 0.43475M - \frac{1877.4}{M},$$

$$\ln p_c = -0.13408 + 2.5019\rho + \frac{208.46}{M} - \frac{3987.2}{M^2},$$

$$\text{and } m_{\text{SRK}} = 0.48 + 1.574\omega - 0.176\omega^2$$

$$= 0.7431 + 0.0048122M + 0.0096707\rho$$

$$- \left(3.7184 \times 10^{-6}\right)M^2. \quad \ldots\ldots\ldots\ldots\ldots (5.80)$$

Note that the use of acentric factor is circumvented by directly calculating the term m used in the α correction term to EOS Constant A.

4. Group C_{7+} into 3 to 12 fractions using equal-weight fractions in each group; use weight-average mixing rules.
5. Calculate volume-translation parameters for C_{7+} fractions to match specific gravities; pure component c values are taken from Peneloux *et al.*[52]
6. All hydrocarbon/hydrocarbon BIP's are set to zero. SRK BIP's given in Chap. 4 are used for nonhydrocarbon/hydrocarbon pairs.

The two recommended C_{7+} characterization procedures outlined previously for the PR EOS and SRK EOS are probably the best currently available (other EOS characterizations, such as the Redlich-Kwong EOS modified by Zudkevitch and Joffe,[56] and some three-constant characterizations should provide similar accuracy but are not significantly better). Practically, the two characterization procedures give the same results for almost all PVT properties (usually within 1 to 2%). With these EOS-characterization procedures, we can expect reasonable predictions of densities and Z factors (± 1 to 5%), saturation pressures (± 5 to 15%), gas/oil ratios and formation volume factors (± 2 to 5%), and condensate-liquid dropout (± 5 to 10% for maximum dropout, with poorer prediction of tail-like behavior just below the dewpoint).

The recommended EOS methods are less reliable for prediction of minimum miscibility conditions, near-critical saturation pressure and saturation type (bubblepoint or dewpoint), and both retrograde and near-critical liquid volumes. Improved predictions can be obtained only by tuning EOS parameters to accurate PVT data covering a relatively wide range of pressures, temperatures, and compositions (see Sec. 4.7 and Appendix C).

5.7 Grouping and Averaging Properties

The cost and computer resources required for compositional reservoir simulation increase substantially with the number of compo-

nents used to describe the reservoir fluid. A compromise between accuracy and the number of components must be made according to the process being simulated (i.e., according to the expected effect that phase behavior will have on simulated results). For example, a detailed fluid description with 12 to 15 components may be needed to simulate developed miscibility in a slim-tube experiment. With current computer technology, however, a full-field simulation with fluids exhibiting near-critical phase behavior is not feasible for a 15-component mixture. The following are the main questions regarding component grouping.

1. How many components should be used?
2. How should the components be chosen from the original fluid description?
3. How should the properties of pseudocomponents be calculated?

5.7.1 How Many and Which Components To Group. The number of components used to describe a reservoir fluid depends mainly on the process being simulated. However, the following rule of thumb reduces the number of components for most systems: group N_2 with methane, CO_2 with ethane, *iso*-butane with *n*-butane, and *iso*-pentane with *n*-pentane. Nonhydrocarbon content should be less than a few percent in both the reservoir fluid and the injection gas if a nonhydrocarbon is to be grouped with a hydrocarbon.

Five- to eight-component fluid characterizations should be sufficient to simulate practically any reservoir process, including (1) reservoir depletion of volatile-oil and gas-condensate reservoirs, (2) gas cycling above and below the dewpoint of a gas-condensate reservoir, (3) retrograde condensation near the wellbore of a producing well, and (4) immiscible and miscible gas-injection. Coats[57] discusses a method for combining a modified black-oil formula with a simplified EOS representation of separator oil and gas streams. The "oil" and "gas" pseudocomponents in this model contain all the original fluid components in contrast to the typical method of grouping where each pseudocomponent is made up of only selected original components.

Lee *et al.*[58] suggest that C_{7+} fractions can be grouped into two pseudocomponents according to a characterization factor determined by averaging the tangents of fraction properties M, γ, and J_a plotted vs. boiling point.

Whitson[2] suggests that the C_{7+} fraction can be grouped into N_H pseudocomponents given by

$$N_H = 1 + 3.3 \log(N - 7), \quad \ldots\ldots\ldots\ldots\ldots\ldots \quad (5.81)$$

where N = carbon number of the heaviest fraction in the original fluid description. The groups are separated by molecular weights M_I given by

$$M_I = M_{C_7}\left(M_N / M_{C_7}\right)^{1/N_H}, \quad \ldots\ldots\ldots\ldots\ldots\ldots \quad (5.82)$$

where $I = 1,..., N_H$. Molecular weights, M_i, from the original fluid description ($i = 7,..., N$) falling within boundaries M_{I-1} to M_I are included in Group I. This method should only be used when C_{7+} fractions are originally separated on a carbon-number basis and for N greater than ≈ 20.

Li *et al.*[59] suggest a method for grouping components of an original fluid description that uses K values from a flash at reservoir temperature and the "average" operating pressure. The original mixture is divided arbitrarily into "light" components (H_2S, N_2, CO_2, and C_1 through C_6) and "heavy" components (C_{7+}). Different criteria are used to determine the number of light and heavy pseudocomponents. Li *et al.* also suggest use of phase diagrams and compositional simulation to verify the grouped fluid description (a practice that we highly recommend).

Still other pseudoization methods have been proposed[60,61]; Schlijper's[61] method also treats the problem of retrieving detailed compositional information from pseudoized (grouped) components. Behrens and Sandler[62] suggest a grouping method for C_{7+} fractions based on application of the Gaussian-quadrature method to continuous thermodynamics. Although a simple exponential distribution is used with only two quadrature points (i.e., the C_{7+} fractions are grouped into two pseudocomponents), Whitson *et al.*[27] show that the method is general and can be applied to any molar-distribution model and for any number of C_{7+} groups.

In general, most authors have found that broader grouping of C_{7+} as C_7 through C_{10}, C_{11} through C_{15}, C_{16} through C_{20}, and C_{21+} is substantially better than splitting only the first few carbon-number fractions (e.g., C_7, C_8, C_9, and C_{10+}). Gaussian quadrature is recommended for choosing the pseudocomponents in a C_{7+} fraction; equal-mass fractions or the Li *et al.*[59] approach are valid alternatives.

5.7.2 Mixing Rules. Several methods have been proposed for calculating critical properties of pseudocomponents. The simplest and most common mixing rule is

$$\theta_I = \frac{\sum_{i\in I} z_i \theta_i}{\sum_{i\in I} z_i}, \quad \ldots\ldots\ldots\ldots\ldots\ldots \quad (5.83)$$

where θ_i = any property (T_c, p_c, ω, or M) and z_i = original mole fraction for components ($i = 1,..., I$) making up Pseudocomponent I. Average specific gravity should always be calculated with the assumption of ideal solution mixing.

$$\gamma_I = \frac{\sum_{i\in I} z_i M_i}{\sum_{i\in I}\left(z_i M_i/\gamma_i\right)}. \quad \ldots\ldots\ldots\ldots\ldots\ldots \quad (5.84)$$

Pedersen *et al.*[55] and others suggest use of weight fraction instead of mole fraction. Wu and Batycky's[63] empirical mixing-rule approach uses both the molar- and weight-average mixing rules and a proportioning factor, F, to calculate p_{cI}, T_{cI}, and ω_I.

$$\theta_I = \sum_{i\in I} \phi_i \theta_i, \quad \ldots\ldots\ldots\ldots\ldots\ldots \quad (5.85)$$

where θ_I represents p_{cI}, T_{cI}, and ω_I and ϕ_i = average of the molar and weight fractions,

$$\phi_i = F\theta_i z_i + (1 - F)\theta_i w_i$$

$$\text{and } w_i = \frac{z_i M_i}{\sum_{j=1}^{N} z_j M_j}, \quad \ldots\ldots\ldots\ldots\ldots\ldots \quad (5.86)$$

with $0 \leqq F \leqq 1$.

A generalized mixing rule for BIP's can be written

$$k_{IJ} = \sum_{i\in I}\sum_{j\in J} \phi_i \phi_j k_{ij}, \quad \ldots\ldots\ldots\ldots\ldots\ldots \quad (5.87)$$

where ϕ_i is also given by Eq. 5.86.

On the basis of Chueh and Prausnitz's[54] arguments, Lee-Kesler[13] proposed the mixing rules in Eqs. 5.88 through 5.92.

$$v_{cI} = \left[\frac{1}{8}\sum_{i\in I}\sum_{j\in J} z_i z_j \left(v_{ci}^{1/3} + v_{cj}^{1/3}\right)^3\right] \Big/ \left(\sum_{i\in I} z_i\right)^2, \quad \ldots \quad (5.88)$$

$$T_{cI} = \left[\frac{1}{8 v_{cI}} \sum_{i\in I}\sum_{j\in J} z_i z_j \left(T_{ci} T_{cj}\right)^{1/2}\left(v_{ci}^{1/3} + v_{cj}^{1/3}\right)^3\right] \div \left(\sum_{i\in I} z_i\right)^2, \quad \ldots\ldots\ldots\ldots\ldots\ldots \quad (5.89)$$

$$\omega_I = \left(\sum_{i\in I} z_i \omega_i\right) \Big/ \left(\sum_{i\in I} z_i\right), \quad \ldots\ldots\ldots\ldots\ldots\ldots \quad (5.90)$$

$$Z_{cI} = 0.2905 - 0.085\omega_I, \quad \ldots\ldots\ldots\ldots\ldots\ldots \quad (5.91)$$

$$\text{and } p_{cI} = \frac{Z_{cI} R T_{cI}}{v_{cI}}. \quad \ldots\ldots\ldots\ldots\ldots\ldots \quad (5.92)$$

TABLE 5.9—EXAMPLE STEPWISE-REGRESSION PROCEDURE FOR PSEUDOIZATION TO FEWER COMPONENTS FOR A GAS CONDENSATE FLUID UNDERGOING DEPLETION

Original Component Number	Original Component	Step 1	Step 2	Step 3	Step 4	Step 5
1	N_2	$N_2 + C_1$*	$N_2 + C_1$	$N_2 + C_1$	$N_2 + C_1 + CO_2 + C_2$*	$N_2 + C_1 + CO_2 + C_2$
2	CO_2	$CO_2 + C_2$*	$CO_2 + C_2$	$CO_2 + C_2$	$C_3 + i\text{-}C_4 + n\text{-}C_4 + i\text{-}C_5 + n\text{-}C_5 + C_6$*	$C_3 + i\text{-}C_4 + n\text{-}C_4 + i\text{-}C_5 + n\text{-}C_5 + C_6$
3	C_1	C_3	C_3	$C_3 + i\text{-}C_4 + n\text{-}C_4$*	F_1	F_1
4	C_2	$i\text{-}C_4$	$i\text{-}C_4 + n\text{-}C_4$*	$i\text{-}C_5 + n\text{-}C_5 + C_6$*	F_2	$F_2 + F_3$*
5	C_3	$n\text{-}C_4$	$i\text{-}C_5 + n\text{-}C_5$*	F_1	F_3	
6	$i\text{-}C_4$	$i\text{-}C_5$	C_6	F_2		
7	$n\text{-}C_4$	$n\text{-}C_5$	F_1	F_3		
8	$i\text{-}C_5$	C_6	F_2			
9	$n\text{-}C_5$	F_1	F_3			
10	C_6	F_2				
11	F_1	F_3				
12	F_2					
13	F_3					
		Regression Parameters				
k_{ij}		1, 9, 10, and 11	1, 7, 8, and 9	1, 5, 6, and 7	1, 3, 4, and 5	1, 3, and 4
Ω_a		1	4	3	1	3
Ω_b		1	4	3	1	3
Ω_a		2	5	4	2	4
Ω_b		2	5	4	2	4

*Indicates the grouped pseudocomponents being regressed in a particular step.

Lee *et al.*[58] and Whitson[2] consider an alternative method for calculating C_{7+} critical properties based on the specific gravities and boiling points of grouped pseudocomponents.

Coats[57] presents a method of pseudoization that basically eliminates the effect of mixing rules on pseudocomponent properties. The approach is simple and accurate. Coats requires the pseudoized characterization to reproduce exactly the volumetric behavior of the original reservoir fluid at undersaturated conditions. This is achieved by ensuring that the mixture EOS constants A and B are identical for the original and the pseudoized characterizations. First, pseudocritical properties (p_{cI}, T_{cI}, and ω_I) are estimated with any mixing rule (e.g., Kay's[64] mixing rule). Then Ω_{aI} and Ω_{bI} are determined to satisfy the following equations.

$$\Omega_{aI} = \frac{\left[\sum_{i\in I}\sum_{j\in J} z_i z_j a_i a_j \left(1 - k_{ij}\right)\right] \Big/ \left(\sum_{i\in I} z_i\right)^2}{\left(R^2 T_{cI}^2 / p_{cI}\right)\alpha_I(T_{rI}, \omega_I)}$$

$$\text{and } \Omega_{bI} = \frac{\left(\sum_{i\in I} z_i b_i\right) \Big/ \left(\sum_{i\in I} z_i\right)}{\left(RT_{cI}/p_{cI}\right)\beta_I(T_{rI}, \omega_I)}, \quad \ldots\ldots\ldots\ldots\ldots\ldots (5.93)$$

$$\text{where } a_i = \Omega_{ai}\frac{R^2 T_{ci}^2}{p_{ci}}\alpha_i(T_{ri}, \omega_i)$$

$$\text{and } b_i = \Omega_{bi}\frac{RT_{ci}}{p_{ci}}\beta_i(T_{ri}, \omega_i). \quad \ldots\ldots\ldots\ldots\ldots\ldots (5.94)$$

Ω_{ai} and Ω_{bi} may include previously determined corrections to the numerical constants Ω_a^o and Ω_b^o. This approach to determining pseudocomponent properties, together with Eq. 5.87 for k_{IJ}, is surprisingly accurate even for VLE calculations. Coats also gives an analogous procedure for determining pseudocomponent v_{cI} for the LBC[24] viscosity correlation.

Coats' approach is preferred to all the other proposed methods. It ensures accurate volumetric calculations that are consistent with the original EOS characterization, and the method is easy to implement.

5.7.3 Stepwise Regression. A reduced-component characterization should strive to reproduce the original complete characterization that has been used to match measured PVT data. One approach to achieve this goal is stepwise regression, summarized in the following procedure.

1. Complete a comprehensive match of all existing PVT data with a characterization containing light and intermediate pure components and at least three to five C_{7+} fractions.

2. Simulate a suite of depletion and multicontact gas-injection PVT experiments that cover the expected range of compositions in the particular application.

3. Use the simulated PVT data as "real" data for pseudoization based on regression.

4. Create two new pseudocomponents from the existing set of components. Use the pseudoization procedure of Coats to obtain Ω_{aI} and Ω_{bI} values, and use Eq. 5.87 for k_{IJ}.

5. Use regression to fine tune the Ω_{aI} and Ω_{bI} values estimated in Step 4; also regress on key BIP's, such as $(N_2 + C_1) - C_{7+}$, $(CO_2 + C_2) - C_{7+}$, and other nonzero BIP's involving pseudocomponents from Step 4.

6. Repeat Steps 4 and 5 until the quality of the characterization deteriorates beyond an acceptable fluid description. **Table 5.9** shows an example five-step pseudoization procedure.

In summary, any grouping of a complete EOS characterization into a limited number of pseudocomponents should be checked to ensure that predicted phase behavior (e.g., multicontact gas injection data, saturation pressures, and densities) are reasonably close to the predictions for the original (complete) characterization. Stepwise regression is the best approach to determine the number and

properties of pseudocomponents that can accurately describe a reservoir fluid's phase behavior. If stepwise regression is not possible, standard grouping of the light and intermediates ($N_2 + C_1$, $CO_2 + C_2$, i-$C_4 + n$-C_4, and i-$C_5 + n$-C_5) and Gaussian quadrature for C_{7+} (or equal-mass fractions) is recommended; a valid alternative is the Li *et al.*[59] method. The Coats[57] method (Eqs. 5.93 and 5.94) is always recommended for calculating pseudocomponent properties.

References

1. Yarborough, L.: "Application of a Generalized Equation of State to Petroleum Reservoir Fluids," *Equations of State in Engineering and Research,* K.C. Chao and R.L. Robinson Jr. (eds.), Advances in Chemistry Series, American Chemical Soc., Washington, DC (1978) **182,** 386.
2. Whitson, C.H.: "Characterizing Hydrocarbon Plus Fractions," *SPEJ* (August 1983) 683; *Trans.*, AIME, **275.**
3. Pedersen, K.S., Thomassen, P., and Fredenslund, A.: "SRK-EOS Calculation for Crude Oils," *Fluid Phase Equilibria* (1983) **14,** 209.
4. Craft, B.C., Hawkins, M., and Terry, R.E.: *Applied Petroleum Reservoir Engineering*, second edition, Prentice-Hall Inc., Englewood Cliffs, New Jersey (1991).
5. McCain, W.D. Jr.: *The Properties of Petroleum Fluids*, second edition, PennWell Publishing Co., Tulsa, Oklahoma (1990).
6. Katz, D.L. and Firoozabadi, A.: "Predicting Phase Behavior of Condensate/Crude-Oil Systems Using Methane Interaction Coefficients," *JPT* (November 1978) 1649; *Trans.*, AIME, **265.**
7. Austad, T. *et al.*: "Practical Aspects of Characterizing Petroleum Fluids," paper presented at the 1983 North Sea Condensate Reservoirs and Their Development Conference, London, 24–25 May.
8. Chorn, L.G.: "Simulated Distillation of Petroleum Crude Oil by Gas Chromatography—Characterizing the Heptanes-Plus Fraction," *J. Chrom. Sci.* (January 1984) 17.
9. MacAllister, D.J. and DeRuiter, R.A.: "Further Development and Application of Simulated Distillation for Enhanced Oil Recovery," paper SPE 14335 presented at the 1985 SPE Annual Technical Conference and Exhibition, Las Vegas, Nevada, 22–25 September.
10. *Designation D158, Saybolt Distillation of Crude Petroleum, Annual Book of ASTM Standards*, ASTM, Philadelphia, Pennsylvania (1984).
11. *Designation D2892-84, Distillation of Crude Petroleum (15.Theoretical Plate Column), Annual Book of ASTM Standards*, ASTM, Philadelphia, Pennsylvania (1984) 8210.
12. Kesler, M.G. and Lee, B.I.: "Improve Predictions of Enthalpy of Fractions," *Hydro. Proc.* (March 1976) **55,** 153.
13. Lee, B.I. and Kesler, M.G.: "A Generalized Thermodynamic Correlation Based on Three-Parameter Corresponding States," *AIChE J.* (1975) **21,** 510.
14. Riazi, M.R. and Daubert, T.E.: "Simplify Property Predictions," *Hydro. Proc.* (March 1980) 115.
15. Maddox, R.N. and Erbar, J.H.: *Gas Conditioning and Processing—Advanced Techniques and Applications*, Campbell Petroleum Series, Norman, Oklahoma (1982) **3.**
16. Organick, E.I. and Golding, B.H.: "Prediction of Saturation Pressures for Condensate-Gas and Volatile-Oil Mixtures," *Trans.*, AIME (1952) **195,** 135.
17. Katz, D.L. *et al.*: *Handbook of Natural Gas Engineering*, McGraw-Hill Book Co. Inc., New York City (1959).
18. Riazi, M.R. and Daubert, T.E.: "Analytical Correlations Interconvert Distillation-Curve Types," *Oil & Gas J.* (August 1986) 50.
19. Riazi, M.R. and Daubert, T.E.: "Characterization Parameters for Petroleum Fractions," *Ind. Eng. Chem. Res.* (1987) **26,** 755.
20. Robinson, D.B. and Peng, D.Y.: "The Characterization of the Heptanes and Heavier Fractions," Research Report 28, Gas Producers Assn., Tulsa, Oklahoma (1978).
21. Riazi, M.R. and Daubert, T.E.: "Prediction of the Composition of Petroleum Fractions," *Ind. Eng. Chem. Proc. Des. Dev.* (1980) **19,** 289.
22. Pedersen, K.S., Thomassen, P., and Fredenslund, A.: "Thermodynamics of Petroleum Mixtures Containing Heavy Hydrocarbons. 1. Phase Envelope Calculations by Use of the Soave-Redlich-Kwong Equation of State," *Ind. Eng. Chem. Proc. Des. Dev.* (1984) **23,** 163.
23. Pedersen, K.S., Thomassen, P., and Fredenslund, A.: "Thermodynamics of Petroleum Mixtures Containing Heavy Hydrocarbons. 2. Flash and PVT Calculations with the SRK Equation of State," *Ind. Eng. Chem. Proc. Des. Dev.* (1984) **23,** 566.
24. Lohrenz, J., Bray, B.G., and Clark, C.R.: "Calculating Viscosities of Reservoir Fluids From Their Compositions," *JPT* (October 1964) 1171; *Trans.*, AIME, **231.**
25. Whitson, C.H.: "Effect of C_{7+} Properties on Equation-of-State Predictions," paper SPE 11200 presented at the 1982 SPE Annual Technical Conference and Exhibition, New Orleans, 26–29 September.
26. Whitson, C.H.: "Effect of C_{7+} Properties on Equation-of-State Predictions," *SPEJ* (December 1984) 685; *Trans.*, AIME, **277.**
27. Whitson, C.H., Andersen, T.F., and Søreide, I.: "C_{7+} Characterization of Related Equilibrium Fluids Using the Gamma Distribution," *C_{7+} Fraction Characterization,* L.G. Chorn and G.A. Mansoori (eds.), Advances in Thermodynamics, Taylor & Francis, New York City (1989) **1,** 35–56.
28. Brulé, M.R., Kumar, K.H., and Watansiri, S.: "Characterization Methods Improve Phase-Behavior Predictions," *Oil & Gas J.* (11 February 1985) 87.
29. Hoffmann, A.E., Crump, J.S., and Hocott, C.R.: "Equilibrium Constants for a Gas-Condensate System," *Trans.*, AIME (1953) **198,** 1.
30. Abramowitz, M. and Stegun, I.A.: *Handbook of Mathematical Functions*, Dover Publications Inc., New York City (1970) 923.
31. Haaland, S.: "Characterization of North Sea Crude Oils and Petroleum Fractions," MS thesis, Norwegian Inst. of Technology, Trondheim, Norway (1981).
32. Watson, K.M., Nelson, E.F., and Murphy, G.B.: "Characterization of Petroleum Fractions," *Ind. Eng. Chem.* (1935) **27,** 1460.
33. Watson, K.M. and Nelson, E.F.: "Improved Methods for Approximating Critical and Thermal Properties of Petroleum," *Ind. Eng. Chem.* (1933) **25,** No. 8, 880.
34. Jacoby, R.H. and Rzasa, M.J.: "Equilibrium Vaporization Ratios for Nitrogen, Methane, Carbon Dioxide, Ethane, and Hydrogen Sulfide in Absorber Oil/Natural Gas and Crude Oil/Natural Gas Systems," *Trans.*, AIME (1952) **195,** 99.
35. Søreide, I.: "Improved Phase Behavior Predictions of Petroleum Reservoir Fluids From a Cubic Equation of State," Dr.Ing. dissertation, Norwegian Inst. of Technology, Trondheim, Norway (1989).
36. *Technical Data Book—Petroleum Refining*, third edition, API, New York City (1977).
37. Rao, V.K. and Bardon, M.F.: "Estimating the Molecular Weight of Petroleum Fractions," *Ind. Eng. Chem. Proc. Des. Dev.* (1985) **24,** 498.
38. Benedict, M., Webb, G.B., and Rubin, L.C.: "An Empirical Equation for Thermodynamic Properties of Light Hydrocarbons and Their Mixtures, I. Methane, Ethane, Propane, and n-Butane," *J. Chem. Phys.* (1940) **8,** 334.
39. Reid, R.C.: "Present, Past, and Future Property Estimation Techniques," *Chem. Eng. Prog.* (1968) **64,** No. 5, 1.
40. Reid, R.C., Prausnitz, J.M., and Polling, B.E.: *The Properties of Gases and Liquids*, fourth edition, McGraw-Hill Book Co. Inc., New York City (1987) 12–24.
41. Roess, L.C.: "Determination of Critical Temperature and Pressure of Petroleum Fractions," *J. Inst. Pet. Tech.* (October 1936) **22,** 1270.
42. Cavett, R.H.: "Physical Data for Distillation Calculations-Vapor-Liquid Equilibria," *Proc.*, 27th API Meeting, San Francisco (1962) 351.
43. Nokay, R.: "Estimate Petrochemical Properties," *Chem. Eng.* (23 February 1959) 147.
44. Pitzer, K.S. *et al.*: "The Volumetric and Thermodynamic Properties of Fluids, II. Compressibility Factor, Vapor Pressure, and Entropy of Vaporization," *J. Amer. Chem. Soc.* (1955) **77,** No. 13, 3433.
45. Edmister, W.C.: "Applied Hydrocarbon Thermodynamics, Part 4: Compressibility Factors and Equations of State," *Pet. Ref.* (April 1958) **37,** 173.
46. Hall, K.R. and Yarborough, L.: "New, Simple Correlation for Predicting Critical Volume," *Chem. Eng.* (November 1971) 76.
47. Kesler, M.G., Lee, B.I., and Sandler, S.I.: "A Third Parameter for Use in Generalized Thermodynamic Correlations," *Ind. Eng. Chem. Fund.* (1979) **18,** No. 1, 49.
48. Twu, C.H.: "An Internally Consistent Correlation for Predicting the Critical Properties and Molecular Weights of Petroleum and Coal-Tar Liquids," *Fluid Phase Equilibria* (1984) No. 16, 137.
49. Peng, D.Y. and Robinson, D.B.: "A New-Constant Equation of State," *Ind. Eng. Chem. Fund.* (1976) **15,** No. 1, 59.
50. Whitson, C.H.: "Critical Properties Estimation From an Equation of State," paper SPE 12634 presented at the 1984 SPE/DOE Symposium on Enhanced Oil Recovery, Tulsa, Oklahoma, 15–18 April.
51. Brulé, M.R. and Starling, K.E.: "Thermophysical Properties of Complex Systems: Applications of Multiproperty Analysis," *Ind. Eng. Chem. Proc. Des. Dev.* (1984) **23,** 833.

52. Peneloux, A., Rauzy, E., and Freze, R.: "A Consistent Correction for Redlich-Kwong-Soave Volumes," *Fluid Phase Equilibria* (1982) **8,** 7.
53. Jhaveri, B.S. and Youngren, G.K.: "Three-Parameter Modification of the Peng-Robinson Equation of State To Improve Volumetric Predictions," *SPERE* (August 1988) 1033; *Trans.*, AIME, **285.**
54. Chueh, P.L. and Prausnitz, J.M.: "Calculation of High-Pressure Vapor–Liquid Equilibria," *Ind. Eng. Chem.* (1968) **60,** No. 13.
55. Pedersen, K.S., Thomassen, P., and Fredenslund, A.: "Characterization of Gas Condensate Mixtures," *C_{7+} Fraction Characterization,* L.G. Chorn and G.A. Mansoori (eds.), Advances in Thermodynamics, Taylor & Francis, New York City (1989) **1.**
56. Zudkevitch, D. and Joffe, J: "Correlation and Prediction of Vapor-Liquid Equilibrium with the Redlich-Kwong Equation of State," *AIChE J.* (1970) **16,** 112.
57. Coats, K.H.: "Simulation of Gas-Condensate-Reservoir Performance," *JPT* (October 1985) 1870.
58. Lee, S.T. *et al.*: "Experiments and Theoretical Simulation on the Fluid Properties Required for Simulation of Thermal Processes," *SPEJ* (October 1982) 535.
59. Li, Y.-K., Nghiem, L.X., and Siu, A.: "Phase Behavior Computation for Reservoir Fluid: Effects of Pseudo Component on Phase Diagrams and Simulations Results," paper CIM 84-35-19 presented at the 1984 Petroleum Soc. of CIM Annual Meeting, Calgary, 10–13 June.
60. Newley, T.M.J. and Merrill, R.C. Jr.: "Pseudocomponent Selection for Compositional Simulation," *SPERE* (November 1991) 490; *Trans.*, AIME, **291.**
61. Schlijper, A.G.: "Simulation of Compositional Processes: The Use of Pseudocomponents in Equation-of-State Calculations," *SPERE* (September 1986) 441; *Trans.*, AIME, **282.**
62. Behrens, R.A. and Sandler, S.I.: "The Use of Semicontinuous Description To Model the C_{7+} Fraction in Equation of State Calculations," paper SPE 14925 presented at the 1986 SPE/DOE Symposium on Enhanced Oil Recovery, Tulsa, Oklahoma, 23–23 April.
63. Wu, R.S. and Batycky, J.P.: "Pseudocomponent Characterization for Hydrocarbon Miscible Displacement," paper SPE 15404 presented at the 1986 SPE Annual Technical Conference and Exhibition, New Orleans, 5–6 October.
64. Kay, W.B.: "The Ethane-Heptane System," *Ind. & Eng. Chem.* (1938) **30,** 459.

SI Metric Conversion Factors

ft^3/lbm mol	$\times 6.242\ 796$	$E-02 = m^3$/kmol
°F	$(°F-32)/1.8$	$= °C$
°F	$(°F+459.67)/1.8$	$= K$
psi	$\times 6.894\ 757$	$E+00 =$ kPa
°R	5/9	$= K$